SOVIET PHYSICS USPEKHI VOLUME 6, NUMBER 3 NOVEMBER-DECEMBER 1963

*SPARK DETECTORS FOR CHARGED PARTICLES**

M. I. DAĬON and G. A. LEKSIN

Usp. Fiz. Nauk 80, 281-329 (August, 1963)

INTRODUCTION

INTRODUCTION

INTEREST in parallel-plate counters has been evoked by the possibility of using them for very exact measurements of the coordinates of charged-particle trajectories and of small time intervals (for example, in the decay of particles). However, the very first investigations (1948—1953) have shown that owing to the long dead time (0.001—0.001 second) the counters cannot be used to register intense particle currents in accelerators. On the other hand, it has not been possible to produce counters with the large working surface needed for cosmic-ray research. This is why parallel-plate spark counters have not been extensively used heretofore.

During the last two years, new ways in the development of the method of spark counters have been successfully tried in many laboratories of the Soviet Union and abroad, and have disclosed rather wide possibilities of using these counters as track instruments in elementary particle and cosmic ray physics. We have in mind triggered spark counters and various modifications of discharge chambers, which are rapidly finding their way into physical experimentation practice and have become just as widely used as scintillation counters or bubble chambers.

The flow of papers devoted to the method itself and to this application continues to grow. It is therefore time to review the published material and to concentrate on the prospects of the method.

*The article contains a review of papers published up to April 1962 on parallel-plate spark counters (with dc and pulsed supply) and on discharge and spark chambers.

Following a historical sequence, the review begins with a description of parallel-plate spark counters with dc supply (Part I); we have deemed it useful to abstract all the published papers and summarize the decade of research in this field, all the more since many papers are still little known to the large group of physicists and may be of considerable interest in the future as a basis for practical realization of fast particle detectors and for measurements of short time intervals; so far, however, very little attention has been paid to the development of these properties of spark counters.

The bulk of the review (Parts II and III) is devoted to the new most promising trends, which are based on the use of pulsed supplies and the use of the counters as tracking instruments.

In Part IV we summarize briefly the properties of the new tracking instruments, consider the possibility of their application, and report briefly the nature of the physical research in which the new method is being used.

As far as we know, this is the first review published anywhere on this subject. There is no doubt that it contains many inaccuracies, particularly because of the lack of a unified point of view on some of the problems touched upon, ambiguous interpretation of individual experimental facts, and sometimes also the lack of a standardized terminology. We hope, however, that the publication of the review will acquaint experimental physicists more rapidly with a new promising method of elementary-process research and will contribute to further development of this method.

I. SPARK COUNTERS

1. General Description of Spark Counters

In 1948 Keuffel called attention, in an article "Counters with Plane Electrodes," to the possibility of using a gas counter with two plane-parallel electrodes, which constitutes a "faster" charged-particle detector than the cylindrical Geiger-Muller counter. The lag in the discharge in the Geiger-Muller counter following the instant of the charged particle passage is due principally to the drift of the electrons from the point of their production into the higher field near the counter filament, where impact ionization and formation of electron-photon avalanches set in.

In the parallel-plate counter the electric field is homogeneous, and if the potential difference on the plates is sufficiently high the impact ionization can begin at any point of the active volume.

We are interested here in counters in which this process terminates in the formation of a streamer and the occurrence of a spark breakdown*. Usually the breakdown is accompanied by sound. The visual effect is a bright sharply localized spark, which can be readily photographed. The voltage pulse produced by a discharge in the chamber is registered without any amplification, since its amplitude is several thousand volts. This signal can also be received by an antenna located laterally away from the counter.

It must be noted that spark counters can be called "fast" only in the sense of a short delay between the discharge and the instant of passage of the charge particle. It is impossible, however, to use spark counters to register intense particle fluxes, for in order to restore the working conditions after each discharge the voltage must be removed from the counter for a time $T \sim 0.001-0.1$ second (dead time of the counter). In practice this is done by connecting to the counter circuit a quenching resistor or a special electronic quenching circuit [7,8].

The first investigations (1948—1953) were aimed at measuring the discharge delay time. They were stimulated at that time by the great interest in small time intervals involved in particle decay and gamma decay of metastable nuclei. At that time Keuffel [2] advanced the hypothesis that the sparks observed in the counter occur near the trajectories of the charged particles and thus can be used to determine the trajectory coordinates. However, this very important question was investigated in detail only in later research (after 1957), which has demonstrated the great capabilities of spark counters with respect to exact localization of charged-particle trajectories.

Figure 1 shows a counter diagram taken from an earlier paper [9] and the simplest counter circuit. Additional explanations are found in Table I, which summarizes the main structural counter data from many papers.

The counters are filled with various working mixtures (see Table I); in all cases the secondary effects on the cathode, which lead to the occurrence of extraneous sparks as well as other harmful effects, are eliminated by using as one of the components of the working mixture the vapor of an organic substance (alcohol, xylol, butane, and acetone).

2. Counting Characteristic

Figure 2 shows a typical counting characteristic (at $T_\theta = 0.05$ sec) [2]. The abscissas are the counter voltages and the ordinates are the pulses registered per second. The size of the "plateau" of the counter

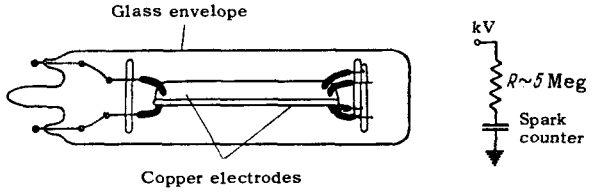

FIG. 1

*See [3] concerning operation in the pre-breakdown mode. We do not touch upon the theory of spark breakdown, which is the subject of many papers and reviews (see, for example, [4-6]).

Table I

Electrode material, electrode dimensions	Distance between electrodes	Working mixture, total pressure	Discharge quenching method	Dead time	Literature
Copper, 35 cm²	2.5 mm	6 mm Hg xylene + argon, 0.5 atm	Quenching circuit	0.05 sec	2
Anode—copper, cathode—various metals, dia. 1/2 – 3 in.	1—10 mm	Argon + butane (10%),, to 3 atm	»	Varying times	8
Copper (rectangular) 50 cm²	2 mm	Saturated alcohol vapor + argon, 60 cm Hg	»	0.01 sec	9
Copper and transparent, 28 cm²	2 mm	Alcohol (saturated vapor) + argon, 34 cm Hg	Not indicated	$5 \cdot 10^{-3}$—10^{-4}	12
Copper foil, 20 cm²	5 mm	40 mm Hg alcohol + 260 mm Hg argon	Quenching resistor	0.01 sec	11
Steel and transparent, 0.75 cm²	0.2 mm	Argon + ether, 3-13 atm	»		17

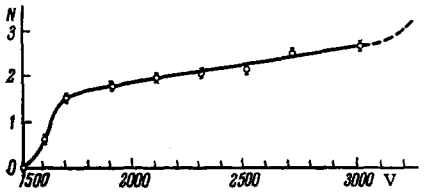

FIG. 2

is approximately 100 V. Similar characteristics are cited in [9-12].

To obtain good counting characteristics (a broad plateau) it is necessary to finish the surfaces and the edges of the plates very carefully, clean them, and keep the distance between them constant.

The authors of [13] were able to greatly increase the counter working region. Their counters had copper electrodes made of thin foil (50 microns) placed 5 mm apart. The electrode dimensions were $5 \times 6 = 30$ cm². A rather complicated procedure was used to purify the electrodes, without which, as claimed by the authors, it was impossible to obtain good counter characteristics.

The working media used in this investigation were mixtures of argon with vapors of different organic substances—alcohol, ether, acetone. The better of the counting characteristics, obtained for a mixture of acetone (35 mm Hg) and argon (265 mm Hg) had a plateau 4 kV wide.

It will be shown below that as the relative overvoltage $\Delta U/U_0$ increases* an improvement takes place in the main characteristics of the counter; its efficiency increases, the deviation of the sparks from the trajectories decreases, and the delay of the discharge relative to the instant of passage of the charge particle is reduced.

*U_0 – voltage corresponding to the start of the count; ΔU – voltage in excess of U_0.

This is precisely why much attention has been paid to obtain as large overvoltages in the counters as possible. In particular, an investigation was made of the dependence of the maximum permissible overvoltage on the composition and pressure of the working mixture for two interelectrode distances, d = 0.25 and 0.5 cm. Figure 3 shows one of the plots obtained [14]. The abscissas are the values of the pressure in the counter, and the ordinates the corresponding overvoltages. Each curve pertains to a definite percentage ratio of acetone to argon in the mixture. It is seen from Fig. 3 that for a specified vapor-gas mixture there exists an optimal value of total pressure and percentage vapor content, giving the best counting characteristic (the largest "plateau"). For the acetone + argon mixture these were found to be 41 cm Hg total pressure and 11.4% vapor content. Finally, it must be emphasized that the counting characteristics depend essentially on the value of T_θ, for the counter plateau increases with this value. In most of the investigations cited above, $T_\theta \sim 0.01$ sec. The low limit of this quantity is apparently 0.001 sec.

The dependence of the value of T_θ on the material used for the counter cathode was investigated in one of the earlier studies [8]; the smallest values of $T_\theta \sim 0.01$ sec were obtained for lead and tin cathodes; these materials, however, are rarely used for electrodes.

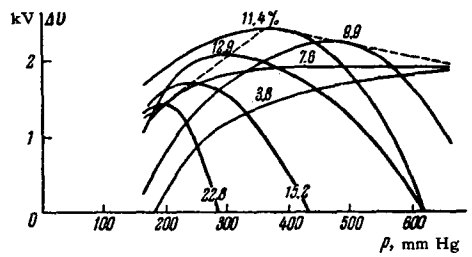

FIG. 3

3. Counter Efficiency

A typical circuit for efficiency measurement is shown in Fig. 4a [13]. The spark counter is placed in a telescope made of Geiger-Muller counters; counters Z_1 and Z_3 are placed perpendicular to Z_2 and Z_4 respectively, so that the particle crosses the working volume of the spark counter in the case of the four-fold coincidence $Z_1 + Z_2 + Z_3 + Z_4 = K_5$. Register 1 gives the number of coincidences K_4 in coincidence block I, while register 2 gives the number of coincidences in block II (where the coincidences of the pulses from the spark counter with the pulses from block I are separated). The spark-counter efficiency is given by the ratio K_5/K_4.

Bella, Franzinetti, and Lee [12] give the following formula for the calculation of the counter efficiency R:

$$R = 1 - \exp(-\nu_0 pd)\left(1 - \frac{\alpha_{ei} d + C}{\alpha d}\right). \quad (1)$$

Here ν_0 is the primary specific ionization—the number of ion pairs produced by a primary particle on one centimeter of path at a pressure of 1 atm, p the pressure (atm), d the interelectrode distance, C = 0.577 (the Euler constant), α_{ei} the gas multiplication number at the potential difference corresponding to the start of the count, and α is the gas multiplication number in the operating mode. From [13,16] it follows that

$$\alpha_{ei}\, d \approx 18 - 20; \quad (2)$$

and neglecting the quantity C we have

$$R \sim 1 - \exp(-\nu_0 pd)\left(1 - \frac{\alpha_{ei}}{\alpha}\right). \quad (3)$$

With increasing overvoltage on the counter, α increases (see [13]) and with it the counter efficiency.

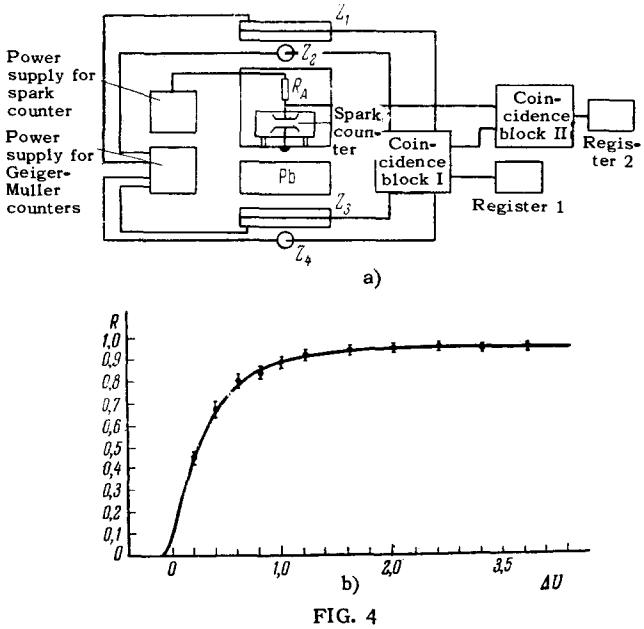

FIG. 4

The first counters [7,8] had a low efficiency for the registration of charged particles ($\sim 10\%$), for owing to poor construction they operated only at low overvoltages. The efficiency of the counters described in the other cited papers is close to 100%.

Figure 4b gives the experimental values of the efficiency obtained for one of the counters [13] (d = 5 mm) at different values of the overvoltage ΔU. The solid curve shows the efficiency as calculated from (1), with the values of α taken from the corresponding measurements of the gas-multiplication numbers in the same mixtures. The counter efficiency is close to 100% over a wide range of overvoltages. If we assume that $\alpha \to \infty$, then for the given counter

$$R = 1 - \exp^{-\nu_0 pd} \sim 0.98.$$

The experimental results are in good agreement with the calculated values.

4. Time Characteristics of Counters

Madansky and Pidd [7,8,11] measured the time intervals between a discharge in a Geiger counter and a spark counter for the same charged particle traversing the two counters. The pulse from the Geiger counter always lags the pulse from the spark counter.* The distribution of the lags is shown in Fig. 5. It is very difficult to measure directly the delay time of the pulses relative to the instant of passage of the charged particle through the spark counter. This is why the relative delay of the pulses from two spark counters was measured in all the investigations.

Keuffel [2] measured the relative delay of the pulses due to a single cosmic-ray particle passing through two counters, one directly on top of the other. If the delay is measured in intervals $\langle \Delta T \rangle$ such that half the cases fall inside the interval $\langle \pm \Delta T \rangle$, then the dependence of the delay on the overvoltage can be represented by the curve of Fig. 6. It is seen therefore that the time lag is greatly decreased at large counter overvoltages. The authors of [11] measured, with an analogous experimental setup, the delay time

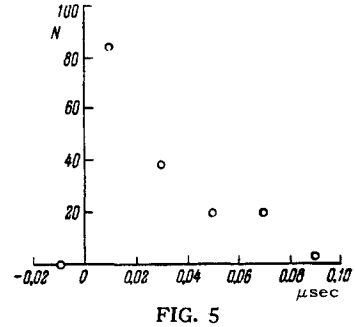

FIG. 5

*The particles (electrons) were made to pass close to the Geiger counter filament (at distances to 1 mm) in order to reduce the time of the secondary electron drift to the filament.

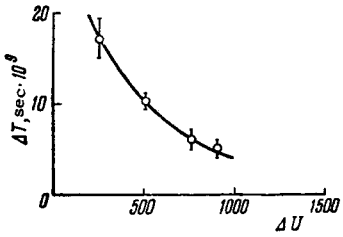

FIG. 6

for two values of counter overvoltage, 300 and 1,000 volts. Their results agree with Keuffel's data.

Robinson [9] gives a histogram of the relative delays in two counters, one located 6 cm over the other. A total of 2,000 events were registered with a counter overvoltage of 500 V. The half-width of the curve approximating the obtained distribution turned out to be 5×10^{-9} sec, approximately in agreement with the preceding investigations.

A further investigation of this question by M. V. Babykin et al [17] and by E. K. Zavoĭskiĭ and G. E. Smolkin [18] has shown that the delays of the discharges in spark counters can be greatly reduced by reducing the distance between counter electrodes. They succeeded in producing and investigating counters in which the interelectrode distance was 0.2 mm (the counters had round electrodes of 10 mm dia and were filled with a mixture of argon and saturated ether vapor at 13 atm total pressure.

The relative delay of the pulses was measured in two closely located counters used to register $\gamma\gamma$ coincidences from Co^{60}. The measurement method was based on registering with an electron-optical converter (EOC) the light flashes accompanying the spark breakdowns.

The histogram given in [18] for the relative delays is appreciably narrower than the histogram obtained in the earlier investigations, with a half-width of 10^{-10} sec. The same authors show a microphotograph of a time-scanned spark image obtained with the aid of the EOC. On the basis of the photographs it can be concluded that the spark duration in the counters ($d = 0.2$ mm) is 2×10^{-9}—3×10^{-9}, and the intensity of the light from the sparks reaches half the maximum value within $\sim 2.5 \times 10^{-10}$ sec.

In a recent paper, Yu. F. Skachkova [19] reports an even narrower delay distribution curve, obtained by further reducing the interelectrode distance and changing the composition of the working mixture.

Figure 7 shows a histogram of the delays in the discharge in counters filled with 0.5 atm O_2 and 20 atm He. The size of the gap is 0.1 mm and the working voltage 4 kV. One division on the abscissa axis of the histogram corresponds to 8×10^{-2} sec. The width of the distribution at half the height is 10^{-11} sec. Detailed information on counter constructions [17-19], the

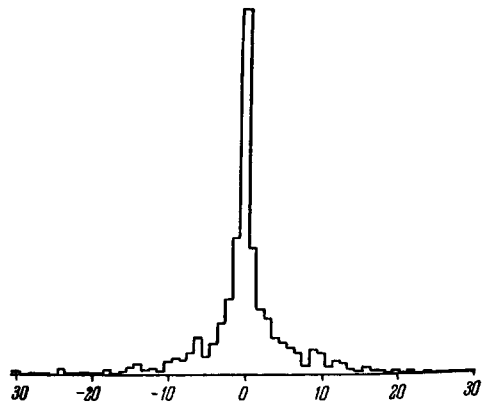

FIG. 7

medium, the characteristics, etc. can be found in the original papers.

Thus, spark counters can be used to measure small time intervals, down to 10^{-9}—10^{-11} sec, but their capabilities in this respect depend strongly on the power supply, the width of the interelectrode gap, the medium, and other parameters.

5. Accuracy of Particle Trajectory Coordinate Measurements

As noted above, the idea that the spark observed in the counter during the passage of a charged particle is produced near the particle trajectory, was advanced already in Keuffel's first paper, but 10 years were to elapse before this question was first subjected to a quantitative study, in [10].

To this end, a telescope consisting of three spark counters, the circuit of which is shown in Fig. 8b, was used. The original connection of the counters is shown in Fig. 8a. A capacitor C_A is connected to each counter through a tube; when the tube is cut off, the counter operates in the usual mode and the spark brightness is determined by the value of the capacitance C_p. If the charged particle passes through all counters simultaneously, then block 1, which receives the pulses from each counter (from resistor R_L), generates a coincidence pulse which is applied through amplifiers 2, 3, and 4 to the grids of the tubes. The tubes conduct and the capacitors C_A discharge through the corresponding spark channels, greatly increasing the brightness of the sparks. Inasmuch as the shutter of the apparatus is open all the time, these bright sparks are seen against the background of a large number of weak sparks from all the extraneous particles passing through the counter. Under the spark telescope are placed a lead block 10 cm thick and a row of Geiger-Muller counters to select the fast muons passing through the lead. Assume that the sparks in counters 1, 2, and 3 are located at distances x_1, x_2, and x_3 from the particle trajectory, respectively. Then

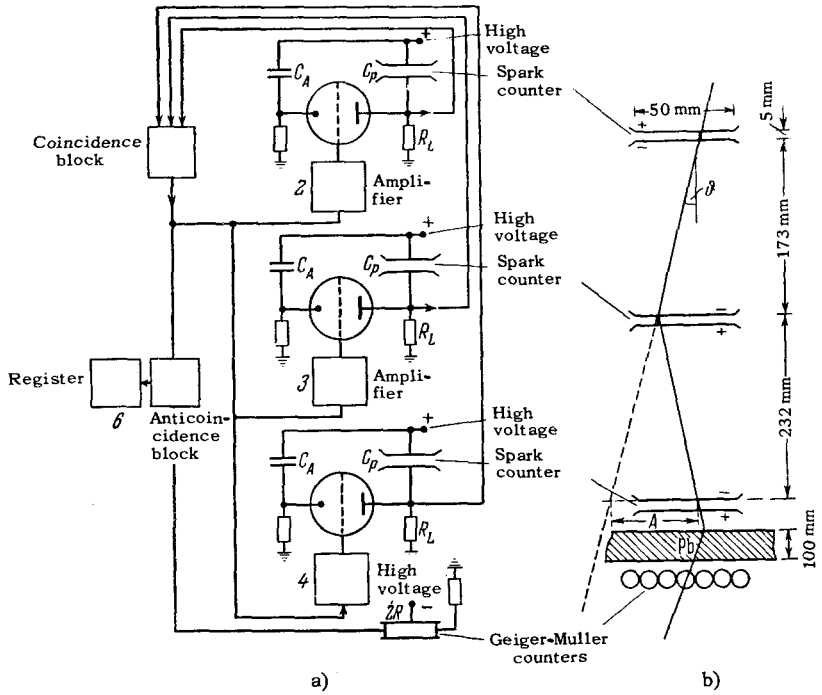

FIG. 8

$$\Delta = \frac{l_2}{l_1} x_1 + x_3 - \left(1 + \frac{l_2}{l_1}\right) x_2. \qquad (4)$$

Here Δ is the experimentally measured deviation of the spark in the lower counter from the line drawn through the sparks in the two other counters. It is obvious that x_1, x_2, and x_3 are independent quantities and $\overline{x_1^2} = \overline{x_2^2} = \overline{x_3^2} = \overline{x^2}$. From (4) we have

$$\overline{\Delta^2} = 2\left[\left(\frac{l_2}{l_1}\right)^2 + \frac{l_2}{l_1} + 1\right]\overline{x^2}.$$

Hence

$$\overline{x^2} = \frac{\overline{\Delta^2}}{2\left[\left(\frac{l_2}{l_1}\right)^2 + \frac{l_2}{l_1} + 1\right]}. \qquad (5)$$

Thus, from the distribution of the values of Δ we can determine the deviation of the sparks from the particle trajectory ($\sqrt{\overline{x^2}}$) of interest to us. The circles in Fig. 9 show the integral distribution of the values Δ obtained in [10]*. The abscissas are the values of Δ, and the ordinates the number of events with deviation larger than Δ. It is useful to consider here some of the physical processes that lead to deviation of the sparks from the trajectories [10].

1) Single-avalanche process. $\nu_0 pd$ pairs of ions are produced on the path of the charged particle in the gas of the counter. If the electron that initiates the cascade is produced at a distance d from the anode such that the Raether condition $\alpha d \geq 20$ is satisfied [16], then a spark breakdown is produced; in this case the spark is produced near the trajectory.

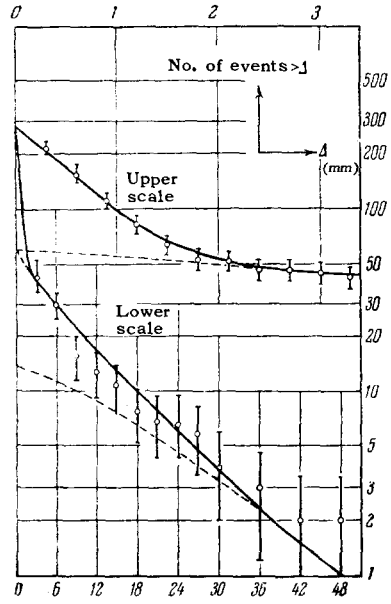

FIG. 9

2) Two-avalanche process. If d_1 is small, so that $\alpha d_1 \approx 16$—17, then the avalanche due to the primary electron does not turn into a spark breakdown. However, a large number of photons are produced in the head of the avalanche and give rise to photoelectrons on the cathode and in the gas of the counter. If $\alpha d_1 \geq 20$ for the latter, then the resultant avalanches grow into a spark breakdown which can be localized to the side of the trajectory.

*The trajectories make a small angle with the direction of the electric field in the counter.

3) Multi-avalanche process. Such a process can be realized, for example, if the time interval between the entry of two particles into the counter is so small that by the time of entry of the second particle the potential on the counter does not have time to reach its working value.

Owing to photoionization, several avalanches for which the critical Raether condition is not satisfied are produced each generating the next. However, in some place near the cathode there can finally occur an avalanche for which this condition is satisfied, and this one turns into a spark breakdown.

4) Production of δ electrons in the counter electrodes. The δ electrons, along with the primary particle, ionize the gas and by the same token can initiate sparks to the side of the trajectory of the primary particle.

5) Cosmic-particle showers. Like δ electrons, extraneous particles can give rise to a spark breakdown to the side of the main trajectory.

According to calculation made by the authors of [10], under the conditions of their experiment the mean-square deviation Δ due to processes 2) and 4) is ~7 mm, while that due to processes 3) and 5) is ~25 mm.

It has turned out that the experimentally obtained distribution of the deviations is well approximated by a curve of the form $\int_{\Delta}^{\infty} W(\Delta)\,d\Delta$ (the solid curve of Fig. 9), where $W(\Delta)$ is equal to the sum of three Gaussian functions with different variances σ_1, σ_2, and σ_3:

$$W(\Delta)=\sum_{1}^{3} W_i(\Delta), \quad W_i(\Delta)=\frac{\alpha_i}{\sqrt{2\pi}\,\sigma_i}\,e^{-\frac{\Delta^2}{2\sigma_i^2}};$$

$$\sigma_1=0{,}8\text{ mm}, \quad \alpha_1=0.78,$$
$$\sigma_2=7\text{ mm}, \quad \alpha_2=0.17,$$
$$\sigma_3=25\text{ mm}; \quad \alpha_3=0.06.$$

78% of all cases constitute small deviations Δ (σ_1 = 0.8 mm) and are essentially due to single-avalanche spark formation in all three counters simultaneously. It follows, therefore, that in each counter ~92% of the sparks ($0.92 \times 0.92 \times 0.92 = 0.78$) are due to the single-avalanche process; for these counters, the mean-square deviation of the sparks from the trajectory is ~0.3 mm [see formula (5)].

With increasing overvoltage on the counter and with decreasing dead time T_θ, the probability of occurrence of a two-avalanche or a multi-avalanche process decreases, and consequently the relative fraction of the single-avalanche processes increases.

The deviations were measured in [14] with a telescope consisting of three and four spark counters, filled with a mixture of acetone and argon (total pressure 350 mm Hg). A very detailed analysis is presented of all the experimental errors and a value $\sqrt{\bar{x}^2}$ = 0.2 mm is given for the mean-square deviation of the spark from the trajectory (disregarding the "tail" of the distribution). It is probable that owing to the large counter overvoltage on the counters better results were obtained in this investigation than in [10].

Finally, a histogram of the deviations, constructed on the basis of a large statistical material, is presented in [15]. Altogether 2056 particles were registered, and in 325 (15.8%) cases the deviation exceeded 1 mm. The results of this investigation agree fully with the deductions of [14].

It is seen from the data presented that a rather large number of false trajectories ("tails" of the distribution) are produced.

In their last paper [20] the authors have shown that the relative number of large deviations ($\Delta > 10$ mm) decreases with increasing thickness of the lead absorber installed over the telescope, in accordance with the shower absorption in this filter as calculated from the Rossi transfer curve. On going from 2 cm to 10 cm of lead, the number of large deviations decreases to almost one-half. This result shows that when several charged particles enter the counter the spark breakdown occurs only in one place, namely where the streamer developed earliest.

In conclusion, let us consider the deviation distribution for trajectories with large inclinations [10].

Figure 10 shows deviation histograms for trajectories moving from left to right and from right to left. To the side of the histograms are diagrams illustrating the measurements of the spark coordinates.

The points selected were those where the sparks crossed the negative electrode in the first case and the positive electrode in the third case, while in the second case the coordinates of the center of the spark

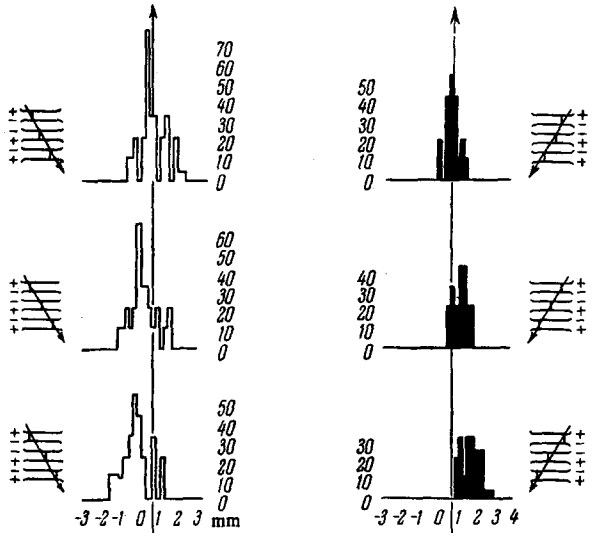

FIG. 10

were measured. The best approximation for the trajectories, giving a symmetrical distribution (about $\Delta = 0$), is obtained in the first case. This result shows that the spark discharge is initiated with a high degree of probability by the electrons produced on the path of the charged particle and located closer to the cathode (since the critical Raether condition $\alpha d = 20$ is satisfied for them with a greater margin).

By special treatment of the electrodes, by precise assembly of the counters, and by selecting the working mixture, it is possible to obtain counters with working area up to ~ 50 cm^2, with good characteristics and a high counting efficiency. An increase in the electrode area entails an increase in the energy released in the spark (since the capacitance of the counter is increased), making it necessary to increase the dead time T_θ so as to reduce the harmful consequences of powerful sparks. The increase in T_θ and the simultaneous increase in the counting rate (which is proportional to the increase in the area) leads to a reduction in efficiency. At the same time it must be noted that even at high values of T_θ (~ 0.5 sec) it is impossible to obtain counters with large working surfaces, for many false sparks not connected with passage of particles through the counter are usually produced.

It is possible that large-area counters can be realized by sectionalizing one of the electrodes [17]; this, incidentally, increases the efficiency of the simultaneous recording of several particles.

To conclude this section, we wish to refer to several investigations in which spark counters were used for physical research. Robinson [9,21] used spark counters to measure the time of flight of a particle through a given path segment and to measure the time of relative delay of particles in showers. Allkofer et al [22] studied the scattering of cosmic-ray muons in lead with the aid of a telescope consisting of three spark counters. Allkofer [15,23] combined a telescope of spark counters with a magnet and measured the momentum spectrum of the muons at sea level up to 6×10^{10} eV/c.

Further applications are connected with new trends in the development of the spark-detector method, to which we turn in the next sections.

II. TRIGGERED SPARK COUNTERS

6. Operating Principle of Triggered Spark Counters

Entirely new capabilities of spark detectors were disclosed by Cranshaw and de Beer [24] who investigated spark counters under triggered pulse conditions. The idea of using a pulsed supply was borrowed by them from Conversi [25,26], who designed an instrument for the registration of charged-particle trajectories in the form of a set of gas-discharge tubes placed in a parallel-plate capacitor*: the tube through which the particle passed glowed if a high voltage pulse was applied to the capacitor electrodes at the instant of particle passage†.

Figure 11 shows a block diagram of the counter connection. The 1 + 2 coincidence pulse, produced when a charged cosmic-ray particle passes through the telescope, triggers a blocking generator, a pulse from which ignites in turn a thyratron that generates a high-voltage pulse across the plates of the spark counter.

It has been found that the gas ionization due to the passing particle persists until the arrival of the voltage pulse on the electrodes (the counter has "memory"); this causes a spark breakdown localized near the particle trajectory.

In this circuit the spark detector unlike the ordinary parallel-plate spark counter, no longer counts all the passing particles, but merely tags with the spark the point through which previously separated particles pass.

In the triggered mode there are no extraneous pulses and associated dead time. In the case of short-duration pulses (10^{-5}—10^{-7} sec), the probability of occurrence of false sparks due to edge effects is decreased, and the spark is produced primarily in the place where the ionization due to the passing particle persists. Thus, the main shortcomings of the spark counter (see Sec. I), which limit its working area service life, have been circumvented.

Not much difficulty is entailed in constructing triggered spark counters with electrode areas amounting to hundreds or even thousands of square centimeters. They are simple to build and operate, and they do not call for such a scrupulous finishing of the electrodes as do ordinary spark counters.

Cranshaw and de Beer investigated counters with metallic electrodes measuring 10×10 cm (interelectrode distance d = 1, 2, and 2.5 mm). The working gas employed was air at atmospheric pressure‡.

The counter supply circuit is shown in Fig. 11. When a pulse is applied from the blocking generator to the thyratron grid, the capacitor C discharges and an exponential voltage pulse is produced across the

*Pulsed supply was used, independently of Conversi, by Tyapkin and by Vishnyakov and Tyapkin [27-28] in experiments with a hodoscope of Geiger-Muller counters. Pulsed supply in the form of a supplementary pulse on top of a high-voltage dc pedestal was used in [20].

†The feasibility of a somewhat different version of the Conversi system has been under extensive discussion recently. We refer here to the experiments of Charpak[29], who observed a glow of neon bubbles moving through transformer oil. Application of a high-voltage pulse produced glow in those bubbles through which a particle passed.

‡In this part we consider only air-filled counters. Counters filled with inert gases have many essential peculiarities and will be considered in the next part.

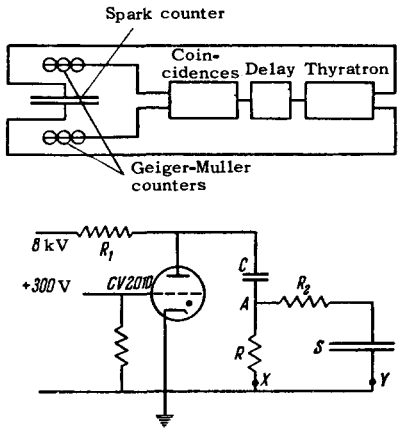

FIG. 11

resistor R, with a time constant RC. This pulse is applied to the counter through resistor R_2 which limits the current through the thyratron. A small clearing field is applied at points X and Y.

Let us consider the initial stage of the operation of the counter. Positive ions (essentially nitrogen ions), and electrons that stick to the oxygen molecules forming negative ions, are produced along the path of the charged particle. The ions of both polarities move to the corresponding plates with velocity v = KV, where V is the magnitude of the clearing field and K is the average ion mobility. In the time interval τ_d elapsed from the start of particle passage to the arrival of the high-voltage pulse (τ_d is the pulse delay time), some of the ions move out of the gap, and not a single ion remains in section X of the gap. We assume that the necessary and sufficient condition for the occurrence of a spark in the spark gap is the presence of at least one ion in the gap between the electrodes up to the instant when the high-voltage pulse reaches some critical value. Two cases are then possible:

a) Ions of either polarity can initiate the discharge.

b) Only ions of one sign can initiate the discharge.

It is obvious that in case a) we have x = vt − d and up to the instant of breakdown the ions remain in a gap s of size

$$s=\begin{cases} 2(d-x), & vt > \frac{d}{2}, \\ d, & vt \leqslant \frac{d}{2}; \end{cases}$$

while in the case b)

$$s = d - vt.$$

The counter efficiency*

$$\varepsilon = 1 - \exp(-ns) \qquad (6)$$

in case a) is then

$$\varepsilon = 1 - \exp[-2n(d-vt)], \quad vt > \frac{d}{2},$$
$$\varepsilon = 1 - \exp(-nd), \quad vt \leqslant \frac{d}{2}; \qquad (7)$$

and in case b)

$$\varepsilon = 1 - \exp[-n(d-vt)], \qquad (8)$$

where n is the specific ionization of the particle.

In air n = 22 ion/cm and the maximum efficiency for a 1 mm gap is 90% in both cases a) and b).

It must be recognized that upon application of the high-voltage pulse the ions are acted upon by an increasing electric field (front of the pulse) in addition to the constant clearing field; the added field also clears the spark gap of ions prior to the start of impact ionization. If we denote by T the time from the start of the pulse to the start of the impact ionization and by $v_i(t)$ the instantaneous velocity of the ions at the time interval T, then the displacement of the ion must be written in more general form as

$$v\tau_d \pm \int_0^T v_i(t)\,dt; \qquad (9)$$

The formula for the efficiency will be in the general case

$$\varepsilon = 1 - \exp\left[-n(d) - v\tau_d \pm \int_0^T v_i(t)\,dt\right]. \qquad (10)$$

The sign of the integral depends on the relative polarities of the high-voltage pulse and the clearing field, since the front of the pulse can displace the ions in the same direction as the clearing field (minus sign) or in the opposite direction (plus sign). The function $v_i(t)$ depends on the parameters of the leading front of the pulse and consequently on many quantities: the chamber capacitance C_C, R_2, C, R, the internal resistance $R_i(t)$ of the thyratron, etc.

The contributions of the individual terms to the exponent of formula (10), and consequently also the roles of the individual parameters, will be made clear in the following.

7. Counting Characteristic

The counting characteristic of a triggered spark discharge gives the dependence of the charged-particle registration efficiency on the amplitude of the high-voltage pulse on the counter (in practice—on the value of the high voltage on the thyratron anode).

The efficiency of a triggered counter is customarily defined as the ratio of the number of events when passage of a particle is accompanied by a spark discharge to the total number of passing particles. In practice, the efficiency is determined by visually counting the sparks, by counting the crackles accompanying the spark breakdown with a microphone [30],

*The formula gives the probability in the sense of Poisson, of finding at least one ion in a gap of size s (the average number of of ions is ns). Other conditions for the occurrence of the discharge are considered in Part I.

or by receiving with an antenna a signal induced by the breakdown; the number of passing particles is determined from the number of operations of the triggering telescope or thyratron. Figure 12 shows a typical counting characteristic (d = 1 mm) obtained [24] at fixed values of the clearing field (+12 V), delay time (6 μsec), and limiting resistance (100 ohms). The width of the "plateau" of the counter is 2,000 V, and the efficiency on the plateau is in good agreement with the calculated value (~92%). A control experiment in which the voltage pulses were applied to a counter at arbitrary instants of time, not connected with the passage of charged particles, showed that the number of accidental sparks is approximately 1%. It was also shown that the variation of the pulse duration (RC) in a range of 10^{-7}—10^{-4} sec did not affect the counter efficiency.

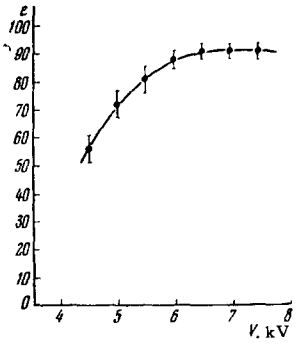

FIG. 12

When the interelectrode distance is increased to 2.0—2.5 mm, the counter efficiency reaches 98—99%, and the working voltage increases to 15—20 kV. A characteristic feature is that the field intensity at which the plateau is reached is 70 kV/cm. It is apparently determined by the condition under which the electrons break away from the oxygen molecules in the air. Indeed, the electron to oxygen molecule binding energy is 0.34 V and when E/p ~ 90 V/cm-mm Hg the electrons should break away from the molecules [6]. This is precisely the value corresponding to the conditions of the cited investigation

$$\frac{E}{p} = \frac{70\,000\ \text{V}}{760\,\text{mm Hg} \cdot \text{cm}} \sim 92 \frac{\text{V}}{\text{cm} \cdot \text{mm Hg}}.$$

Counting characteristics for various pressures were obtained by Bayukov, Leksin and Suchkov [31] for d = 2 mm, R_1 = 0, V = 0, and τ_d = 0.5 μsec. They show that the start of the "plateau" moves towards the higher voltages with increasing pressure (see curves 1 and 2 on Fig. 13). With decreasing pressure, the slope of the plateau increases, and when p = 150—200 mm Hg the operating region disappears completely; the character of the discharge changes from clearly localized sparks to a large number of thin sparks in the region where the particles pass. At low gas pressures (~20 mm Hg) diffused glow of the entire counter ensues, and further decrease in the pressure causes the entire evacuated volume to glow.

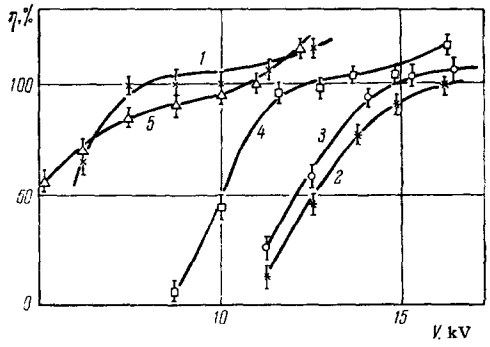

FIG. 13. Counting charactertistic.

$R_1 = 0$, $V = 0$, $\tau = 0.5$ μsec

Curve	Gas	p, mm Hg	d, mm
1	Air	400	2
2	»	760	2
3	Argon	760	6
4	»	400	6
5	»	400	4

In conclusion we wish to call attention to an interesting but very little investigated property of the spark counter, namely its ability to distinguish (statistically) between particles having different ionizing abilities.* Indeed, in accordance with formula (6), the counter efficiency depends on the quantity ns, and at low values of ns we have in first approximation ε ~ ns. If a particle passes in succession through a large number of spark gaps, ε can be estimated directly:

$$\varepsilon = \frac{\text{number of gaps in which breakdown occurred}}{\text{total number of spark gaps}}$$

and the value of n estimated therefrom. In practice, a spark counter of low efficiency (with respect to relativistic particles) or a system consisting of several counters can be used to separate the strongly ionizing particles against the background of relativistic particles, or particle beams (say the core of a shower) against the background of individual particles. Some data on the dependence of the efficiency of the air spark gap on the ionizing ability of the particles were obtained by the group of Bayukov and Leksin. The counting characteristics for the registration of the particles in the hard component of cosmic rays (minimum ionization) and β particles from a radioactive source with average energy 300 keV yield efficiencies of 70 and nearly 100% on the plateau, respectively.

8. Time Characteristics

We consider here the question of the "memory" and of the "dead" time of the counter. It follows

*Similar to the low-efficiency Geiger-Muller counters [32].

from (6) and (7) that the counter ineffectiveness $\sigma = 1 - \varepsilon$ increases exponentially with increasing v, that is with increasing clearing field V:

$$\sigma = 1 - \varepsilon = \exp[-n(d - vt)]$$

$$\ln \sigma = -n(d - vt). \quad (11)$$

This linear dependence of $\ln \sigma$ on V is confirmed by the experimental results [24] shown in Fig. 14a, where σ (the ordinates in logarithmic scale) is plotted against the clearing field V_{cl} for three values of the supply-pulse delay time τ_d—67, 36 and 15 μsec. What is striking is, first, the fact that the counters have a large "memory": when the high-voltage pulse is delayed by even several dozen microseconds the charged particles are still registered with high efficiency. Extrapolating the results obtained to the point $\sigma = 1$, that is, to $\varepsilon = 0$, we readily find the value of K from the relation d = KVt. Its values are 22 cm/sec-V at 650 V/cm and at a delay of 67 μsec, 24.4 for 1150 V/cm and 36 μsec, and 33 for 2,000 V/cm and 15 μsec (the error in the determination of K is ±1 cm/sec-V). These values do not contradict the known data on the mobility of ions in gases, thus indicating that the "memory" of air-filled spark counters has an ionic mechanism.

Figure 14b shows the same data as in Fig. 14a, but the abscissas are the values of $\nu t/d$. The same figure shows two lines, 1 and 2, calculated from formulas (7) and (8) respectively. The experimental results lie quite definitely on the single straight line (2), so that we can conclude that spark discharges are initiated by ions of the same polarity. If, in addition, we take the deduction of the preceding section into consideration, we can trace the following pattern of discharge development in the counter.

Positive ions (essentially nitrogen) and negative oxygen ions are produced along the path of the charged particle; the negative oxygen ions are the result of sticking of primary electrons to the oxygen molecules. Prior to the high-voltage pulse, both types of ions move in the clearing field towards the corresponding electrodes. In the strong electric field produced by the voltage pulse, the electrons break away from the oxygen molecules and acquire an acceleration sufficient to produce electron-photon avalanches which then turn into streamers. The positive ions, on the other hand, can not cause further ionization under these conditions. The large "memory" of the counters is due to the sticking of the electrons to the molecules, whose mobility is appreciably reduced and which remain for a long time in the working volume of the counter.

Let us determine in greater detail the value of τ—the numerical measure of the "memory" of the spark counter. We assume that τ is numerically equal to a delay τ_d such that the efficiency of registration of the charged particles decreases to one-half*. Figures 14 and 25 show that τ depends on the value of the clearing field, and the larger V the smaller this dependence. In small clearing fields τ reaches several dozens or even hundreds of microseconds [24,31]. It is easy to see that τ depends also on many other parameters, for example, d, p, etc. These dependences can be easily predicted qualitatively, but they have not been investigated experimentally for air-filled counters.

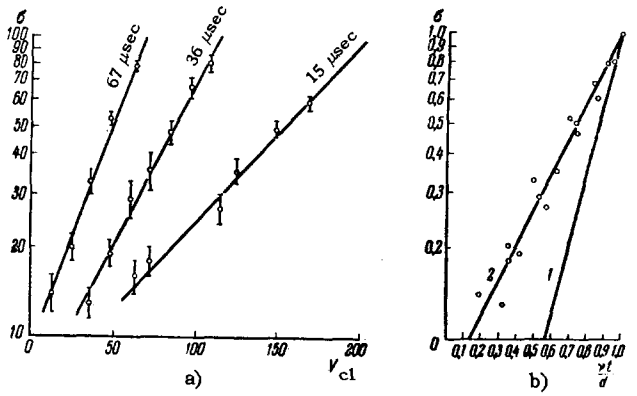

FIG. 14.

Let us consider now the question of the "dead" time of the counter, since this quantity characterizes along with the "memory" the possibility of registering particular events. The "dead" time T_θ is usually defined as the time necessary to restore the working conditions following a spark breakdown. When voltage pulses are applied to the counter with a repetition period smaller than T_θ, false breakdowns occur, as a rule at the location of the first breakdown. One of the estimates of the value of T_θ was obtained by Bayukov and Leksin in the following experiment: periodic pulses were fed to a spark counter from a generator; these pulses were not connected with the traversing particles. The pulse repetition frequency for which any breakdown in the chamber gave rise to uninterrupted breakdowns following each high-voltage pulse was then determined. The value of T_θ depends on many parameters; p, V, d, etc., but these relationships were not investigated as such. For the cited parameters, $T_\theta \sim 0.1$ sec.

We have disregarded above the front of the high-voltage pulse, because its duration in the experiments considered up to now was short, on the order of several dozen nanoseconds. However, it is easy to disclose the clearing action of the leading front of the pulse (see Sec. 1 of this part). Figure 15

*The question of defining τ was considered also in a symposium on spark chambers[33] held at the Argonne National Laboratory in 1961. In addition to the definition presented here, a somewhat different $\tau = \tau_d$ was considered there, for which the registration efficiency of a charged particle was decreased by a factor e.

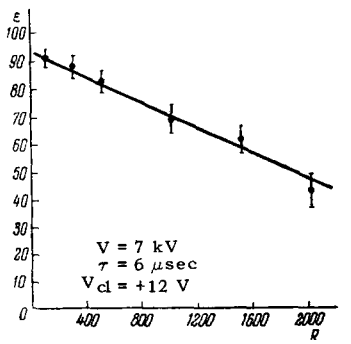

FIG. 15

shows the dependence of the efficiency on the limiting resistance R_2. The counter efficiency decreases with increasing R_2. A similar drop in efficiency is observed if the counter capacitance is increased and not R_2. Analogous conclusions were arrived at by the authors of [31]. This result is attributed to the action of the pulse front: before reaching the critical value necessary for the electron to become detached from the oxygen molecule, the pulse accelerates the ions and exerts an action analogous to that of the clearing field. With increasing R_2C_2, the duration of the action of the field on the ion increases, and consequently the counter efficiency decreases.

9. The Counter as a Track Instrument. The Counter in a Magnetic Field. Simultaneous Registration of Several Particles

Inasmuch as the triggered spark counter is no longer a particle counter in the usual sense of the word, but is intended to determine the location of a trajectory, its most important characteristic is the accuracy with which the trajectory is localized.

This question was investigated by Daĭon, Volynskiĭ and Potapov [30] in a study devoted to the construction of a spark-counter telescope in a magnetic field. For better utilization of the magnet gap and for more accurate measurement of the spark coordinates, the authors constructed counters with transparent electrodes, through which the sparks were photographed. The electrodes employed were glass plates 1.7 and 5 mm thick, coated with a conducting $SnCl_2$ film. The interelectrode distance was 2 mm and the plate area 200 × 100 mm. The counters were assembled in flat Plexiglas boxes and filled with an air and argon mixture (30 cm Hg) plus saturated vapor of pirydine or alcohol to a total pressure of one atmosphere.

A telescope of three spark counters was placed in the electromagnet gap in order to measure the momenta of the cosmic particles. The diagram of the instrument is shown in Fig. 16. Here 1, 2 and 3 are the camera lenses; shown further are reflecting mirrors, three rows of spark counters, and rows of triggering Geiger counters located below them; in plane B, the particle trajectory is bent very little by

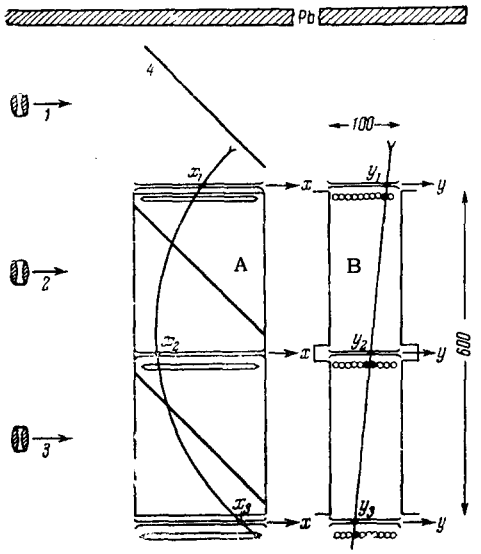

FIG. 16

the magnetic field and follows a straight line. Therefore, by measuring in this plane the deviation of the lower spark from the line drawn through the sparks in the two upper counters, it is possible to determine the mean-square deviation of the spark from the trajectory in each counter. We have mentioned this method in part I of the present review. It has turned out that for single trajectories* the bulk of the cases (~90%) clusters about small deviations, ~1.3 mm. For these cases the mean-square deviation is 0.4 mm†. We can therefore conclude that for 96.5% of the single sparks produced in the given counter (0.956 × 0.965 × 0.965 = 0.9) the mean-square deviation from the trajectory is 0.18 mm [see formula (5) of part I]. Thus, the trajectory in a telescope with several spark gaps can be determined with high degree of reliability and accuracy. Of great practical significance is the use of spark counters in a magnetic field. The investigation of the counter parameters in a magnetic field, made by the authors of [30], is therefore of interest. Under the conditions of their experiment (magnetic field of 6300 Gauss, counter clearing field 40 V/cm) no visible change was observed in the spark size and brightness; the counter efficiency also remained the same as before.

The question of the spark deviation in a magnetic field was investigated under the same conditions and it was shown that if it exists at all, it does not exceed 0.1 mm.

*In approximately 2-10% of the cases not one but several sparks are produced in the counter. This effect depends, in particular, on the resistivity of the plates; it increases with increasing resistivity, for then the individual parts of the plates are better decoupled electrically (see below).

†We note that the contribution from the particle distance in the central counter is relatively small.

Later, in 1961—1962, Daĭon, Knyazev and Akopyan have shown that all of the counter characteristics listed in the present section remain practically unchanged even under more "stringent" experimental conditions: a magnetic field of 10,000 Gauss, a clearing field of 400 V/cm, and a high-voltage pulse lagging the instant of particle passage by 30 μsec.

In 1961, the same group investigated the accuracy with which the particle trajectory can be retraced by using a spark counter in open air. It was shown that in open air the number of false sparks in the spark gap increased, and for the sparks of the main group the scatter in the deviations from the charged-particle trajectory increased. The mean-square deviation reached in this case 1.6 mm. A similar result was obtained by Thompson and Wolfendale [34] *.

The broadening of the distribution of the number of sparks as a function of their deviation from the trajectory is apparently the result of the secondary photoeffect on the cathode (see Sec. 4 of Part I), since addition of argon and organic vapors to the working medium decreases the scatter of the streamers by several times [30].

The most important problem in the use of the spark counter as a track detector is the possible simultaneous registration of several particles or the simultaneous registration of one spark by many counters connected in parallel. It is shown in [31] that in a spark chamber consisting of four spark gaps with d = 2 mm and s = 10 × 4 cm^2, filled with air at 1 atm, the spark breakdown is produced as a rule only in one gap and in one point in this gap. The breakdown occurs apparently where the electron first breaks away from the oxygen molecule and where the streamer is produced earliest. The development of the discharge at this point produces a drop in the counter plate potential, and this prevents formation of the remaining streamers.

This property of air counters is their greatest shortcoming. For example, in the registration of particles accompanied by an extraneous background, or when residual ionization due to preceding particles is present in the gas, sparks located to the side of the trajectory may be produced in the air counter. These apparently explain, in part, the already mentioned "tails" in the deviation distribution. It must be noted that if several air spark gaps are used, they can be fed from a single thyratron. For this purpose it is necessary to connect decoupling resistances [30,31] or inductances [31] in series with at least one of the electrodes of each spark gap. The purpose of these decoupling resistances is to slow down the decrease in the voltage across the gaps which have not yet broken down, so that the time during which the voltage remains above the breakdown value is longer than the time fluctuations of the start of the breakdown.

We have been considering air-filled spark counters. In [31] there is brief mention of counters filled with CO_2 and N_2. It is shown that they are similar to air counter with respect to registration of many particles and the presence of a long memory. It is probably that the "memory" mechanism has here, too, an ionic character, although it must be borne in mind that the probability of the electrons sticking to the CO_2 molecules is very low. It is possible that the results obtained depend to some degree on the impurities in the gas.

10. Remarks Concerning Construction Features

Usually in air-filled spark counters the electrodes are spaced d = 2 mm apart, and must therefore, be parallel within at least ~ 0.05 mm. A good method for adjusting the electrode spacing is to use calibrated washers, which can be installed not only at the edges of the electrodes, but also in the center. However, the material used for the washers is of great importance [30]; for example, in the case of glass washers breakdown can occur along the surface. Good results are obtained with washers made of polystyrene or teflon [30], probably owing to the low dielectric constants of these materials. In the case of relatively small interelectrode distances and large electrode areas, certain difficulties can arise in connection with the photography of sparks in several narrow spark gaps. We have already mentioned (Sec. 4) a system developed [30] for photography through transparent electrodes. Bayukov, Leksin, and Lesina proposed to fix the spark position with the aid of coordinate paper: graph paper was placed in the spark gap, in which a hole 0.1 mm in diameter was burned by the spark at the breakdown location (provided the current was sufficiently high). It was shown that introduction of the graph paper did not affect adversely the counting characteristic. The proposed method is best used if the counter operates in open air and there is free access to the spark gap. There is no doubt that in many cases the possibility of working in open air does in itself greatly simplify the counter construction. In order to obtain high efficiency of registration of several particles, it is possible to make one of the counter electrodes in the form of a mosaic, with decoupling resistors connected between the individual parts of the mosaic. This idea was realized in practice by Daĭon, Knyazev and Akopyan.

11. New Variant of Triggered Pulse Supply for Counters

Trumper, [20] continuing to develop the ideas of the German researchers (see Part I), proposed a triggered pulse power supply for spark counters, some-

*Recently Daĭon, Knyazev, and Solodnikov greatly improved this result by increasing the overvoltage on the counter and by increasing the interelectrode distance.

what different from the Cranshaw and de Beer circuit*. Trumper's circuit is shown in Fig. 17. Here S_1 and S_2 are two ordinary spark counters, connected in a coincidence circuit. The three investigated counters D_1, D_2, and D_3 (electrode area 5 × 5 cm, d = 5 mm, acetone (35 mm Hg) plus argon with a total pressure 30—50 cm Hg) are maintained at a constant potential somewhat lower than the static breakdown potential. Consequently, the avalanches produced in the counters by the passage of charged particles do not develop into spark breakdowns. At the instant of an $F_1 + F_2$ coincidence an additional short-duration high-voltage pulse is applied to counters D_1, D_2, and D_3, producing spark breakdowns in the region of the initial avalanches.

The telescope $D_1D_2D_3$ can in general be triggered, without an extraneous triggering system, by separating the coincidences of the pulses produced in these counters in the pre-breakdown mode [3]. This interesting version of telescope triggering is undoubtedly worthy of attention.

III. DISCHARGE AND SPARK CHAMBERS

12. Introduction

We have shown in the preceding part the extent to which the capabilities of parallel-plate spark counters are expanded by using a triggered pulse supply. However, the success was incomplete, since the "air" counters, which were the first objects of the investigation, still had many serious shortcomings which hindered, in particular, their use in accelerators (see Part II).

One more effort was necessary to complete the groundwork and finally attract the interest of the experimental physicists to the new method. This role was assumed by the paper of Fukui and Mijamoto "New Type of Particle Detector—Discharge Chamber" [35]. What was essentially new in this work was such a seemingly inessential detail as the use of neon (with a small amount of argon added) in place of air as the working medium. However, the result of this substitution turned out to be so important, that one cannot disagree with the claims of the authors that a new particle detector has been developed. Fukui and Mijamoto constructed a system consisting of several spark gaps, in which, as in a multiple-plate cloud chamber, successive sections of the particle trajectory are viewed. This is why the new instrument was called a "chamber."

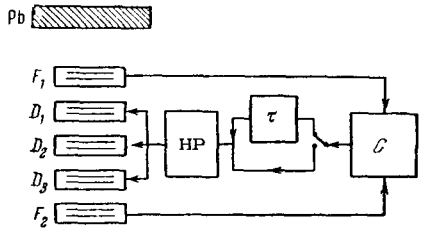

C -- coincidence block
τ — delay block
HP — high-voltage pulse block

FIG. 17

Following the paper by Fukui and Mijamoto, reports were published in the Soviet Union on a somewhat different variant of triggered chambers, filled with inert gases—neon [31,36], argon [31,37,38], helium [31] or a mixture of these gases with organic-compound vapor [38]. Following the accepted terminology, we shall call them "spark chambers." The first reports on spark chambers by foreign authors were made at a conference in Berkeley in August 1960 [39] *.

For a long time the opinion was that spark chambers differed from discharge chambers not only in construction but also in their physical properties. Further accumulation and analysis of experimental data, however, have shown that there is no principal difference between these instruments.

We shall consider discharge and spark chambers separately, after which we shall compare their main characteristics.

13. New Type of Particle Detector—"Discharge Chamber"

The foregoing heading is also the title of the article by Fukui and Mijamoto [35] devoted to a new particle detector, in which the spark discharge is produced along the particle trajectory†. We note here also another important feature which distinguishes the new instrument, from ordinary spark counters, namely the possibility of observing particle showers.

The chamber was assembled of individual flat rectangular glass boxes filled with a working mixture Ne + Ar (0.5%) at atmospheric pressure‡. The inside dimensions of each box were 8.5 × 13 × 2 (or 1) cm. The boxes were placed one on top of the other and separated by electrodes—metal plates or conducting glass plates; in some cases the electrodes used were conducting layers deposited on the outsides of the glass covers; the electrode surface was separated in all cases from the working medium by a dielectric (glass) layer. Figure 18a shows a sketch

*Trumper's paper was published in 1960, following the publication of the papers on discharge and spark counters, reviewed in the following parts of the survey.

*At the same conference, A. I. Alikhanyan and M. S. Kozodaev reported on the work done by Soviet researchers. Much material was considered at the symposium on spark chambers at the Argonne National Laboratory in 1961[33], in which work by Soviet researchers, who obtained by that time analogous experimental data, was not represented.

†The tracing of a discharge along the trajectory of a charged (alpha) particle was first described in [40].

‡Later discharge chambers were also filled with helium[41].

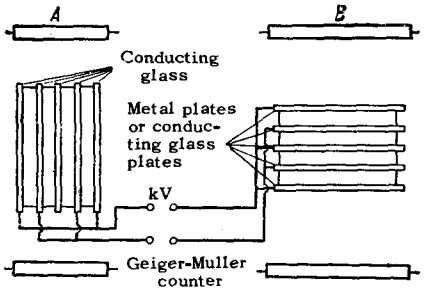

a)

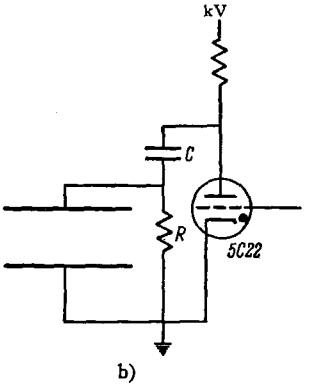

b)

FIG. 18

of a chamber consisting of four boxes, and the low-voltage supply circuit (Fig. 18b). The supply-pulse delay time is one microsecond and RC ~ 0.1 μsec. Figure 19 shows a photograph of the discharges produced in the chamber by passage of a single charged particle. In this case the discharge occurs not along the direction of the external electric field, but at an angle, in the direction of the trajectory of the passing particle.

It turned out that when the angle θ between the trajectory and the direction of the electric field is less than 15°, the sparks have the same slopes in all the segments; in the angle range $15° < \theta < 30°$ a kink in the spark path is sometimes observed, or branching into several channels. At angles $\theta > 60°$ a chain

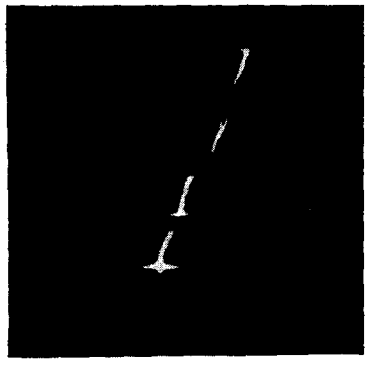

FIG. 19

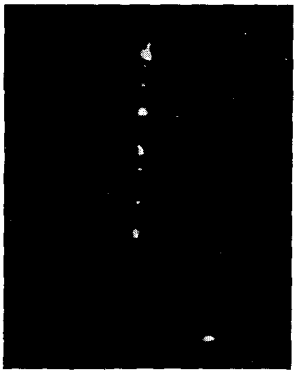

FIG. 20

of sparks is produced along the trajectory. Figure 20 shows a photograph of the discharges occurring when a particle passes along the interelectrode gap, with the plates arranged vertically (see Fig. 18a). The picture was taken through the conducting surfaces of the plates*. It was established that an insensitive zone 2—3 mm wide, in which no discharges were produced, exists near the positive electrode. Table II summarizes the working characteristics of the chamber at the different values of the supply voltage. It can be concluded from these data that the working region is quite broad. Table III lists data on the efficiency of the chamber as a function of the delay of the high-voltage pulse. A sharp decrease in efficiency is observed with increasing delay time, caused by the diffusion of the electrons to the plates.

Pulse delay is accompanied also by a broadening of the discharge column (see Fig. 21 and Table IV). Figure 21 shows a comparison of the observed and calculated broadening under the assumption that the broadening of the column is due to the diffusion of the electrons from the place of their production: the points represent the experimental values and the continuous curve the calculated values. The good agreement between these results indicates that the individual discharges are initiated along the particle path by electrons produced on the path of the primary particle. Finally, it is of interest to determine the number

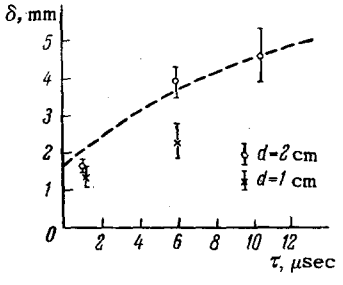

FIG. 21

*The authors do not give a photograph of another projection. A similar photograph in two projections, taken under somewhat different conditions, is shown in Fig. 29.

Table II

Applied voltage (maximum value)	11 kV/2 cm	12 kv/2 cm	13 kV/2 cm, 14 kV/2 cm	15 kV/2 cm
Tracks present	No tracks	Weakly visible tracks appear	Bright tracks	
Discharges not connected with tracks	Discharges appear rarely on the sides of the box	Discharges occur on the sides of the box		False discharges occur in the entire volume
	No discharges occur in boxes through which a charged particle does not pass			

Table III

	Pulse delay time			E_{max}
	1 μsec	6 μsec	10.5 μsec	
Efficiency	~ 100% Good tracks visible on all frames	~ 50% Lightly bent tracks or no tracks visible in half of the frames	~ 10% Accidental discharges seen	13 kV/2 cm
	~ 100%	~ 50%	~ 5%	10 kV/1 cm

Table IV

Pulse delay time	1 μsec	6 μsec	10.5 μsec
Box height 2 cm (13 kV/2 cm)	1.7±0.2 mm	3.9±0.4, mm	4.6±0.7
Box height 1 cm (10 kV/1 cm)	1.4±0.3 mm	2.3±0.5 mm	

Table V

Box height 2 cm	Voltage	13 kV/2 cm			15 kV/2 cm
	Pulse delay time	1 μsec	6 μsec	10.5 μsec	1 μsec
	No. of spark channels per centimeter	1.8±0.3	2.2±0.4	2.9±0.7	2.6±0.3
Box height 1 cm	Voltage	8 kV/1 cm		10 kV/1 cm	
	Pulse delay time	1 μsec		1 μsec	
	No. of spark channels per centimeter	2.4±0.3		2.6±0.4	

of sparks produced per unit path under these conditions. In some respects we have here an analogy with the counting of the drops along the particle path in a cloud chamber. The authors' data are summarized in Table V. It is seen from the table that the number of sparks is approximately 1/10 the number of electrons produced by the primary particle. This effect can be due to many processes, for example, recombination, production of negative ions, and other processes which are considered in[35] only qualitatively*. An important characteristic of the chamber is its dead time T_θ, which determines the possibility of regis-

*It is possible that in the future it will be possible to correlate the number of sparks per unit path with the ionizing ability of the particle.

tration of frequent events; without stopping to discuss how the dead time is determined, we indicate that it amounts to 0.1—0.2 sec.

Let us consider now, following Fukui and Mijamoto, the possible mechanism for the occurrence of a discharge along the particle trajectory.

Passage of the charge particle leaves in the counter a chain of electrons, with each succeeding electron closer to the plate. When a high-voltage pulse is applied, each electron initiates a cascade, and for inclined trajectories an electron cloud of one cascade occurs near the positive-ion cloud of the neighboring cascade. When these clouds are suitably arranged, the electric field between them can become sufficiently strong to cause the further development of the cascades to be governed by this field rather than by the external electric field (which decreases exponentially with time). In the theory of streamer discharges a formula is derived for the field E at a distance x from the center of the head of the cascade:

$$E = \frac{4}{3}\varepsilon\alpha\rho e^{\alpha\delta/x^2},$$

where ε is the electron charge, α the Townsend coefficient, ρ the radius of the avalanche head, and δ the path covered by the avalanche. If it is assumed that in order for cascades to develop along the trajectory the field E_c must be at least equal to the external field E_0, we obtain the equation

$$E_c = \frac{4}{3}\varepsilon\alpha\rho e^{\alpha\delta/x^2} = E_0 e^{-t/10^{-7}},$$

where t is the action time of the external field. Under the conditions of [35] with $t = 5 \times 10^{-8}$ sec, the space-charge field is approximately equal to the external field. Then $\rho = 0.007$ cm.

If we denote by l the average distance between primary electrodes, which is equal to 0.03 cm, then, if $2\rho > l \sin\theta$, the two neighboring clouds will overlap. This gives a critical value $\sin\theta < 0.007/0.03$, corresponding to $\theta \sim 30°$. The fact that at $15 < \theta < 30°$ the discharges do not always follow the trajectories is attributed by the authors of the paper to fluctuations in the development of the cascade and to diffusion of the primary electrons.

Further investigations of discharge chambers were made in Dubna by A. A. Tyapkin (see [39]) and by Govorov et al [42] in experiments with cosmic rays and with a 660-MeV proton beam from an accelerator. The authors developed chambers with long interelectrode gaps, up to 70 mm, and filled with neon at atmospheric pressure and 0.4% argon added. In one of the constructions, the electrode was an electrolyte poured over the surface of an organic-glass box containing the working volume of the chamber. Photographs were obtained of tracks making different angles with the electrodes; typical photographs are shown in Fig. 22.

Figures 22a and b show track photographs of protons passing successively through two chambers, one

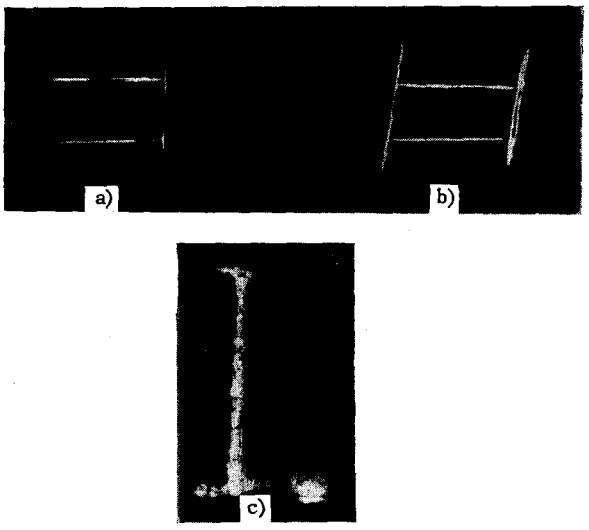

FIG. 22

placed at an angle to the direction of motion of the protons. The track thickness is 2 mm. The maximum angle at which the discharge always passes along the track is 30°. At angles larger than 30°, both normal and distorted tracks were observed. Sometimes satisfactory tracks were observed even at angles close to 50°. The authors note that the maximum angle increases with decreasing gradient of the electric field, with decreasing duration of the pulse, with decreasing front of the high-voltage pulse, with increasing ionizing ability of the particles, and with increasing distance between electrodes. Figure 22b shows a photograph of the track of a particle passing along the electrodes. The photograph was taken through the transparent electrode. In the other projection the track becomes smeared out on going from electrode to electrode. The authors note also smearing of the track perpendicularly to the electric field, owing to secondary discharge columns near the main spark channels.

The time characteristics presented in the paper agree with the data of Fukui and Mijamoto.

14. Spark Chamber. Counting Characteristic of the Spark Chamber

The spark chamber usually constitutes a shelf structure (metallic or glass plates with conducting coatings on both sides), placed in a box filled with inert gas*. Unlike the discharge chamber, the electrodes are in direct contact with the working gas in this case. The interconnection of the plates and the high-voltage pulse supply are exactly the same as used by Fukui and Mijamoto. Figure 23 shows a photograph obtained by Mikhaĭlov, Roinishvili, and Chikovani [36] in a 10-layer spark chamber made up of brass plates measuring 11 × 14 cm and filled with

*Differently constructed variants will be considered below in Sec. 20.

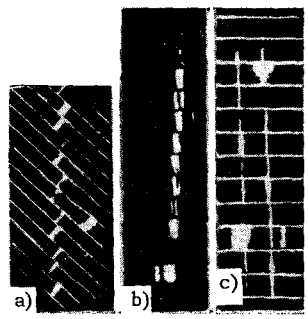

FIG. 23

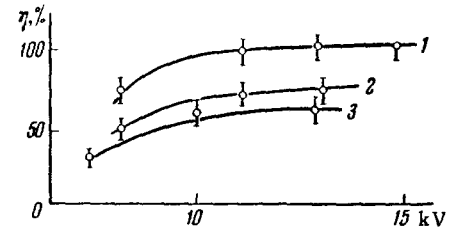

FIG. 24

1—12 pF; 2—1170 pF; 3—2000 pF.

neon "of special purity" to a pressure 1.1 atm. The particle trajectory can be traced by following ten sparks, each 2—3 mm in width (distance between electrodes is 10 mm). The photograph shows that, unlike in the discharge chamber, the development of the discharge in the spark chamber is along the direction of the external magnetic field, although in some segments the sparks do follow the trajectory or exhibit kinks. Similar chambers, filled with inert gases, are widely used and have been described in many papers [31,33,36-39]. We shall consider their main properties below.

The operation of the spark chamber is characterized to a considerable degree by the properties of the individual spark gap, which has the same construction and supply circuit as the air counter (see Fig. 11), and is investigated in an analogous method and from the same point of view. We shall therefore refer frequently to the corresponding section of the preceding part, emphasizing only the principally new features introduced into the operation of the spark chamber by the use of the inert gas as a medium.

The counting characteristic of a spark chamber filled with inert gas is a typical curve with a plateau. It is easy to obtain a chamber efficiency close to 100% and an operating-region width of 3—5 kv. At d = 10 mm and p = 1 atm (these parameters are typical of a large number of investigations), the working region is near ~7 kV for neon and 13 kV for argon, that is, smaller gradients are necessary for argon and neon chambers than for air chambers, for in this case there is no detachment of electrons from the electronegative ions. On the high-voltage side, the plateau is limited by the spontaneous breakdown, which is not connected with the passage of particles (see Part II, Sec. 7). However, if the high-voltage pulse is always connected with the passage of a particle through the chamber, the breakdown will occur at the point of passage of the particle under considerably higher voltages. This effect extends the operating region even more.

The information presented must be regarded as tentative. We already know that the counting characteristic depends on many parameters of the equipment. Figure 13, to which we have already referred in the discussion of the air chambers, shows the counting characteristics for different p and d. Figure 24 shows the counting characteristics for a chamber with a capacitor connected in parallel [43]. We see that reduction of the pressure and of the distance between electrodes, and also increase of the chamber capacitance, lead to a decrease in efficiency. For the same pulse front, $\sim 3 \times 10^{-8}$ sec, the working region disappears completely in the case of a spark chamber with d = 3—4 mm filled with neon or argon at atmospheric pressure. However, an efficiency exceeding 90% was obtained for a chamber using neon at 1.3—2 atmosphere pressure with d = 3 mm.

These phenomena can be described by formula (10), and are connected with the time behavior of the spark chambers, and primarily with the fact that the front of the pulse and the clearing field have time to gather away the electrons from a larger or smaller part of the spark gap prior to the breakdown.

Let us consider a few other details. The amplitude of the high-voltage pulse necessary for normal operation of the spark chamber does not depend strongly on the distance between the electrodes (it varies more slowly than the first power of the distance). From an examination of curves similar to 4 and 5 on Fig. 13, and also from experience with electrodes in the form of round frames with foil stretched over them [31], it can be concluded that even when the gap varies by 5—10% from point to point in the chamber, the chamber efficiency remains close to 100%. The working region decreases in this case. The 5—10% figure is the order of magnitude of the required accuracy in the adjustment of the electrodes, and determines in particular the requirements imposed on the care in stretching the foil, on which waves may be produced by temperature variations.

Brief information concerning chambers filled with helium and xenon are contained in [31,44] and in [45] respectively. A helium chamber with d = 6 mm, p = 760 mm Hg, $V_{cl} = 0$, $\tau = 0.5$ μsec at V = 16 kV had an efficiency of 100%, which dropped to 80% for d = 3 mm, p = 4 atm, and V = 12 kV. For a xenon chamber with d = 7 mm, the efficiency was 90% in the pressure range 0.1—0.2 atm. Mention is made in [44] of a hydrogen-filled spark chamber. With d = 3 mm, V = 12 kV, and a pressure in the range 1—3, the hydrogen chamber had negligible efficiency.

15. Time Characteristics of the Spark Chamber

We have already mentioned the electronic mechanism of memory in spark chambers filled with inert gases. Let us consider the corresponding experimental data.

Figure 25, from the paper of Bayukov et al [31], shows the dependence of the efficiency on the clearing field for a chamber filled with argon at p = 400 mm d = 6 mm (curve 6) and d = 4 mm (curve 7); τ = 0.5 μsec. For comparison, the same figure shows the corresponding curve for a chamber filled with air (curve 1) at p = 760 mm Hg, d = 2 mm and τ = 0.5 μsec. These curves differ greatly, particularly at low clearing fields. The results presented for argon can be readily treated by means of formula (11), as was done for air chambers in Sec. 3 of the preceding chapter. The value $\sim 3 \times 10^{-3}$ cm^2/V-sec obtained for the mobility corresponds to the mobility of the electrons in the gas. Properly speaking, evidence in favor of the electronic memory mechanism is presented even by the relatively short memory time of the spark chambers, which of course depends, as we shall show presently, on many parameters.

Figure 26 shows the dependence of the efficiency on the time delay (Curve 1) for a high-voltage pulse applied to a neon spark chamber (d = 8 mm, p = 1.1 atm, V_{cl} = 0), given in the paper by Mikhaĭlov, Roinishvili and Chikovani [36]. The chamber memory time amounts to several microseconds. Figure 27 shows the corresponding data obtained by Cronin's group [46] in Berkeley. The family of curves was plotted for a neon chamber with different values of clearing fields. Similar information can be found in many papers [39]. An analogous variation is observed for an argon chamber [31,38].

Simultaneous examination of all the published experimental data makes it possible to draw the following conclusions concerning the memory time of spark chambers filled with inert gases.

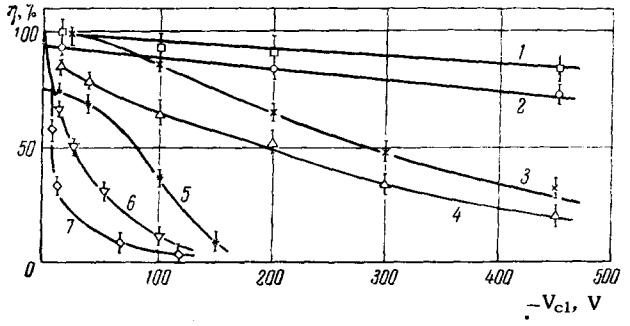

FIG. 25. Efficiency vs. clearing field (V_{cl}).

Curves	Gas	p, mm Hg	τ, μsec	d, mm
1	Air	760	0,5	2
2	»	760	4,0	2
3	»	400	0,5	2
4	»	760	20,0	2
5	»	760	100,0	2
6	Argon	400	0,5	6
7	»	400	0,5	4

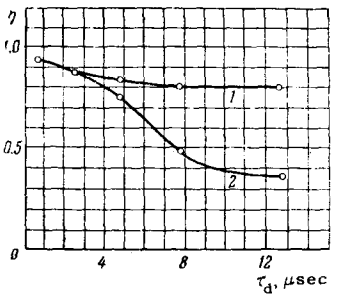

FIG. 26

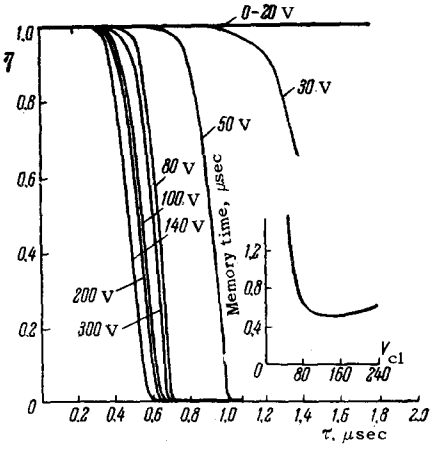

FIG. 27

a) The memory time varies from fractions of a microsecond to ten microseconds, depending on the type and pressure of the gas, distance between electrodes, clearing voltage, etc. The upper limit is determined by the diffusion of the electrons in the gas. The role of the diffusion is also manifest in the broadening and splitting of the spark in the case of long delays of the high-voltage pulse. The lower limit of the memory time has not been investigated, since there are difficulties in applying a high-voltage pulse with sufficiently steep front, $\sim 10^{-8}$ sec, and with a delay time shorter than a fraction of a microsecond. If these difficulties are overcome, we can hope that for some parameters of a spark chamber the memory time will at least be one order of magnitude shorter than that obtained.

b) The memory time decreases with increasing voltage. However, according to Cronin's data (see Fig. 27) for a neon chamber, it has a minimum which is attained at V_{cl} = 150 V. This is apparently connected with the fact that large clearing fields will by themselves start to accelerate the electrons to the atomic excitation energy. At the present time there are no data concerning the memory time for clearing fields exceeding 400 V.

c) The memory time of the chamber decreases with decreasing working pressure.

d) At a fixed gas pressure, the memory time decreases with decreasing distance between electrodes (see for example, curves 6 and 7 on Fig. 25). It is precisely this effect, when $\tau \lesssim \tau_d$, which determines the minimum distance between the electrodes (see the last section). In estimating the influence on d, it is necessary to take into account not only the fact that when this quantity decreases the distance which the electron must cover in order to reach the electrode decreases, but also that, other conditions remaining equal, the capacitance increases and consequently the front of the high-voltage pulse becomes less steep.

e) The character of the dependence of the efficiency of the spark chambers on the delay time for fixed values of p, d, and V is such (see Fig. 27) that for any of the curves given, even at the lowest value of the delay, there is a region with $\sim 100\%$ efficiency. The presence of such a region has great practical importance, since τ_d cannot be made very small. The width of this region depends apparently on the same parameters as the memory time itself.

f) The curves of the chamber efficiency against the delay time, for large values of τ_d, frequently have slowly descending "tails" at the 20—30% level (see, for example, Fig. 26). The "tails" are due apparently to the impurities in the gas filling the chamber. This may be an admixture of a electronegative gas or a gas that ionizes as a result of removal of the excitation from the atom of the main gas, which is in a metastable state. The mechanism of this phenomenon has not been investigated in detail. Addition of uncontrollable impurities to the working gas also gives rise to a scatter in the time characteristics obtained by different workers or even by one and the same group at different times. Thus, curve 2 of Fig. 26 is the same chamber characteristic as represented by curve 1, except that it has been plotted immediately after filling the chamber (whereas the previously presented curve was obtained after several hundred discharges in the chamber, after it has attained sufficient time stability). It is probable that the observed differences are due to gas released from the chamber material (see Sec. 1).

The question of the dead time has been considered in Sec. 3 of Part II. We note merely that in chambers filled with inert gases the dead time can apparently be reduced to 5—10 μsec [33]

Fischer and Zorn [48] measured the time of formation of a spark in a spark chamber filled with inert gases. Detailed dependences of this time on the value of the high-voltage pulse were obtained at different values of d for chambers filled with different gases (argon, neon, helium), with and without addition of alcohol. The time of formation of the spark varies from several microseconds to several hundredths of a microsecond. It decreases rapidly with increasing amplitude of the high-voltage pulse.

16. Simultaneous Registration of Several Particles

We have already seen (see the typical photograph on Fig. 23) that one particle is registered effectively in all the gaps of a multi-layer chamber if the latter are connected in parallel and are fed from one high-voltage source. A spark chamber is also capable of registering several charged particles simultaneously (Fig. 28) [43] (see also [46,47]).

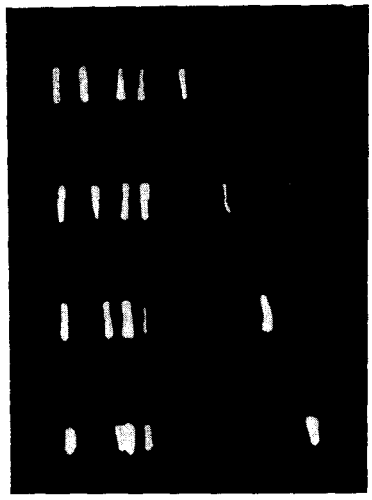

FIG. 28

It is simpler to register one particle in several gaps connected in parallel than it is to register several particles in a single spark gap [43,45]. The reason for it is apparently that the spark gaps are still decoupled from one another. To be sure, this decoupling is much weaker than that required for the operation of air spark chambers, but it is sufficient, inasmuch as the neon and argon chambers have an electronic memory and the fluctuation in the time of the start of the discharge is much smaller. These fluctuations are apparently so small that at sufficiently high voltages it is not only the parallel gaps that are decoupled, but even individual points on the same electrode; the drop in the potential at the point of the electrode where the discharge occurs does not have time to influence appreciably the potential at the point where the second discharge begins to develop, and in any case the potential of the second point also corresponds to the working region.

Meyer and Terwilliger [49] investigated the efficiency of registration of one particle in two parallel gaps with different electrode distances. For d = 11.1 and 12.7 mm, the second gap did not operate at all. However, when decoupling resistances were connected in the leads supplying the pulse to the two chambers, both gaps were made to break down by a single particle, with efficiency $\sim 100\%$. The authors note that a small sag in the electrode in an individual gap (d

Table VI

V_{cl}, V	η_{12}	η_{22}	η_{32}	$\eta_{12}-\sqrt{\eta_{24}}$	$\eta_{12}-\sqrt[3]{\eta_{34}}$
0	1.00±0.01	0.97±0.01	0.91±0.02	0.02±0.02	0.03±0.02
7	1.00±0.01	0.96±0.03	0.89±0.02	0.02±0.02	0.04±0.02
10	1.00±0.01	0.94±0.03	0.86±0.02	0.03±0.03	0.05±0.02

= 9.6 mm) leads to a decrease in the efficiency of registration of the second particle (to 50%). In the same paper are given data on the efficiency of registration of a large number of particles; a decrease in efficiency by 50% is noticed on passage of 20–30 particles simultaneously through the gap. These observations agree with the qualitative picture of simultaneous registration of several particles considered above.

Quantitative data on the efficiency of registration of several particles in one spark gap (d = 10 mm, D = 13 kV) were obtained in [43] for a four-layer neon chamber operating with a meson beam. The corresponding values of the efficiency of registration of one particle and of two or three particles in a single spark gap are summarized in Table VI. If the particles are registered in the gap independently of one another, the efficiency for the registration of two particles is expected to equal the square of the registration efficiency of one particle, that for three particles to equal the cube, etc. In the fifth and sixth columns of the table are listed the differences between the experimentally observed efficiencies and those calculated under this assumption. It is evident that even the registration of three particles cannot be regarded as an independent event.

Spark breakdowns in the chamber differ from one another in the glow intensity. This is apparently connected with fluctuations in the initial stages of the discharge development. The glow intensity depends on the number of sparks, on their mutual placement, etc. The question of the relative intensity of spark glow has not been investigated in detail. It can only be noted that in the case when several particles are registered, the difference in the spark brightness makes it possible to identify the track of a particle in two orthogonal projections.

The question of simultaneous registration of tracks of particles that pass through a chamber at different times has been discussed in a symposium [33]. It has been noted, in particular, that the registration efficiency of the "old" and "new" tracks is different. This question was not investigated in greater detail.

In conclusion, let us stop to discuss the registration of many sparks produced when a particle passes through a chamber at a small angle to the electrode plane. The corresponding results, analogous to those obtained by Fukui and Majamoto (see Sec. 13 of this part), are contained in [37,38]. Figure 29 shows by way of an example a photograph of two projections of a particle track in a five-layer spark chamber with transparent electrodes [37].

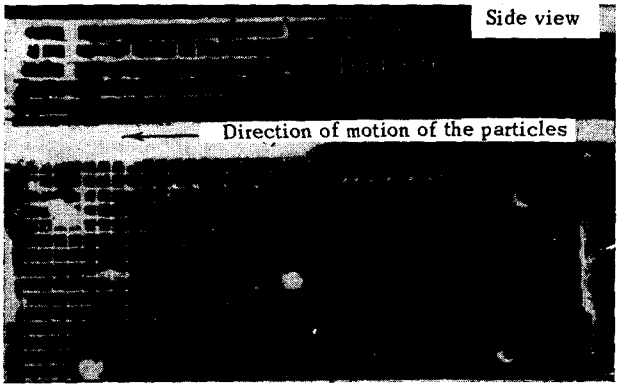

View through the transparent electrodes

FIG. 29

17. Deviation of the Spark from the Particle Trajectory

The most important question is that of the value of the deviation of the streamer from the particle trajectory and the accuracy with which the trajectory of the particle can be reconstituted by observing a chain of sparks in the spark chamber.

Mikhaĭlov et al [36] measured in a ten-layer neon spark chamber (d = 10 mm) the coordinates of the spark centers and drew by the method of least squares straight lines approximating the trajectory. The mean-square deviation of the centers from this line turned out to be σ = 0.22 mm for trajectories that make a small angle θ with the direction of the electric field in the chamber. The distribution of the deviations is shown in Fig. 30. The deviation method (see Part I) was used to determine in a five-layer argon chamber [37] the mean-square deviation of the streamer from the trajectory, $\sigma \sim 0.22$ mm, for trajectories with inclination $\theta < 10°$.*

With increasing slope of the trajectory, the distance from the center of the spark to the trajectory

*The coordinates were measured by determining the points of intersection of the streamer with the negative electrode; where the streamer was bent, in the cases when a straight-line section was observed near the positive electrode, the measurement was based on the point of intersection of the negative electrode with the continuation of the straight-line part of the streamer.

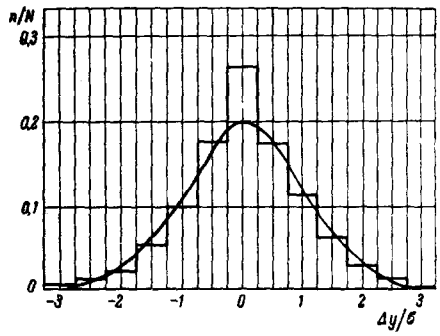

FIG. 30

increases, since the streamer is initiated predominantly by the electrons located closest to the negative electrode (see Sec. 4 of Part I). The authors of [36] obtained a value $\sigma = 1.6$ mm at an angle $\theta \sim 45°$. An analysis has shown that in this case the closest to the approximating line were the points of the sparks situated at a distance s = 0.16d from the negative electrode (for which $\sigma \sim 0.44$ mm). A similar result, $\sigma \sim 0.2$d, was obtained by Rutherglen and Paterson[50] for a seven-layer chamber, filled with a mixture of helium (75%) and argon (25%). These authors have investigated in detail the scatter of the sparks at different slopes of the trajectories[50,51] and different delay times of the high-voltage pulse. As a measure of the scatter they have chosen the quantity δ, which is the distance from the determined spark point to the line joining similar points of the extreme sparks.

The abscissas of Fig. 1 are the deviations (measured by the spark points situated at a distance s = 0.2d from the negative electrode) and the ordinates are the numbers of events (in per cent) having a deviation smaller than δ. The three curves a, b, and c pertain to trajectories that lie in the angle intervals 0—15°, 15—30°, and 30—45°, respectively ($\tau_d = 0.25$ μsec). Comparison of these curves shows that with increasing slope of the trajectory the deviation of the sparks from the trajectory increases. The same figure shows curve d for the angle interval 0—15°; for $\tau_d = 1.6$ μsec it is much less steep than the corresponding curve a, indicating that the deviations increase noticeably with increasing delay time of the high-voltage pulse. The main cause of this is the diffusion of the electrons during the delay time.

For inclined trajectories, in addition, an important role is played by the fluctuations in the position of the initial points of occurrence of the streamer and other factors, for example, the departure of the electrons from the vicinity of the negative electrode to the electrode.

Let us consider now the influence of the electrical clearing field. The clearing field transports the column of electrons produced along the path of the particle to the positive electrode. When the high-voltage pulse (of polarity opposite that of the clearing field) is applied, the streamer is initiated as before by the electrons situated near the negative electrode, but these electrons turn out to be far away from the trajectory. The points closer to the trajectory are now those situated not at a distance s ~ 0.2d from the negative electrode, but at a different distance. For example, a value s = 0.75d is obtained for a 100-V clearing field; however, the curves obtained under the new conditions for distribution of the values of δ (for s = 0.75d) turn out to be identical to the curves a, b, and c of Fig. 31.

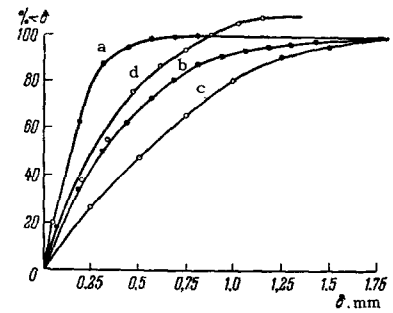

FIG. 31

We have thus considered the influence of some factors on the deviation of the streamer from the trajectory, and have presented numerical values of this quantity for ordinary operating conditions of spark chambers.

More exact values for the specific cases are best obtained directly by means of a control experiment.

In conclusion it must be noted that the scatter of the streamer should depend on the value of the overvoltage on the spark chamber; in the region of low overvoltages at the start of the plateau the scatter can increase noticeably (see Sec. 4 of Part I), but there are still no direct pertinent experimental data. In addition to the papers referred to, there are some communications containing data on the accuracy with which coordinates are measured in spark chambers, and these data are in approximate agreement with those presented. Inasmuch as these communications have not been published, there is no sense in discussing these results in greater detail.

18. Succession of Sparks Along the Particle Track

Borisov et al [38] have shown for the first time that under certain conditions the sparks follow the trajectory of the charged particles in an ordinary spark chamber without a dielectric between the electrodes. The investigations were carried out with a chamber filled with argon at atmospheric pressure or with an argon and alcohol (saturated vapor) mixture at 0.5—1 atm. The interelectrode distance was 10, 12, and 30 mm. Up to particle-trajectory inclinations ~30°, the discharges always followed the particle trajectory (Fig. 32a), but when a 300 pF capacitor was connected in parallel with the chamber (the capacitance of which

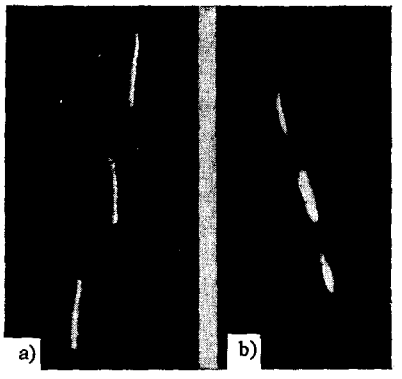

FIG. 32

was 50 pF), step-like tracks replaced the inclined tracks (Fig. 32b). With further increase in the capacitance, the usual discharge picture occurring in spark chambers with small gap, where the discharge is perpendicular to the electrodes, was observed (see Fig. 23).

The succession of the sparks along the track was observed very consistently in spark chambers with large gaps. Thus, [52] reports investigation of chambers with 50—100 mm spark gaps, fed with high-voltage pulses from a Marx discharge generator. It was shown that in these chambers, in a cone ranging in angle from 0 to 40°, the discharge always follows the trajectories of the particles and the chambers register the particle showers effectively. The best results were obtained with chambers filled with neon of high purity. Chikovani et al [53] (Fig. 33), using a telescope of three spark chambers (one with a 100 mm gap and two others with 50 mm gap each) have shown that in a chamber measuring 800 × 400 × 100 mm, the errors in the measurement of the inclination of the trajectory by determining the inclination of the spark is on the order of 10^{-3} radian, that is, the discharge follows very accurately the particle trajectory. Figure 33a shows a photograph of a particle shower obtained in the same chamber.

Another group* investigated a chamber 40 cm high (chamber area 30 × 30 cm, glass walls, electrode area 60 × 60 cm), consisting of two sections of 20 cm each, separated by an aluminum foil 50 microns thick. The chamber was filled with pure neon to a pressure of 650 mm Hg and operated at 55 kV on each section. The upper and lower electrodes of the chamber were layers of $SnCl_2$ (resistance ~100 Ω/cm), deposited on glass. Sparks induced by muons with momentum >1 BeV were photographed (the threshold was set by means of a layer of lead located above the chamber), for which the mean-square multiple scattering angle in the foil was 4×10^{-4} radian. The photography was by means of an RP-53 lens, corrected for the front wall of the chamber, with low optical distortion in the central region of the chamber. The photography scale was 1 : 10. The high-voltage pulse was applied to the chamber from a discharge generator with a lag of 0.6 μsec following the passage of the particles; the pulse rise time was 10^{-8} sec and its duration 10^{-7} sec. Geiger-counter telescopes separated the muons going into an angle 0—8° to the vertical.

Fifteen muon trajectories passing through the central part of the chamber were processed (Fig. 34).

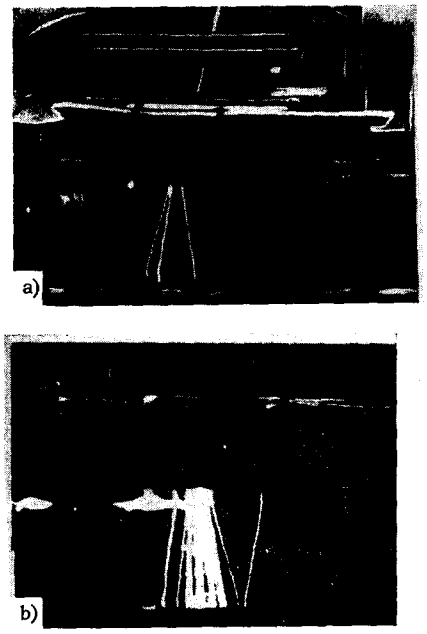

FIG. 33

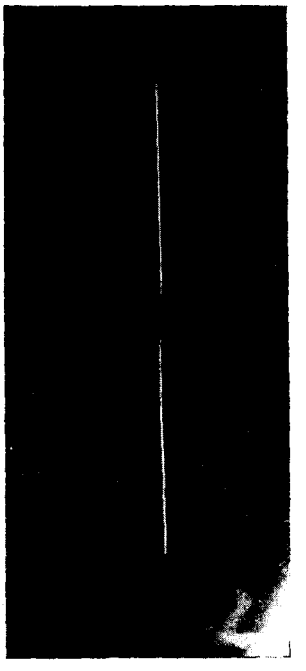

FIG. 34

*V. N. Bolotov, M. I. Daĭon, M. I. Devishev, V. N. Dolgoshein, L. F. Klimanova, V. I. Luchkov, A. P. Shmeleva.

A total of 100 points of the trajectory were measured in the film in each section, and the approximating straight line was drawn by the method of least squares. The angle between these lines in the two sections of the chamber was determined. The mean-square value of the angle, after corrections for distortion, was found to be $(0.65 \pm 0.3) \times 10^{-3}$ rad. If we take into account scattering in the foil, then the mean-square value of the false angle between the tracks in two sections of the chamber amounts to 0.5×10^{-3} rad; these quantities are considerably larger near the chamber walls, apparently owing to the greater inhomogeneity of the electric field in this region.

The authors suggest that in a chamber where the electric field is highly homogeneous the value of the false angle can be decreased. We note that the quality of the tracks in the chamber depends significantly on the pulse parameters.

The data presented concerning the succession of the spark along the particle trajectory can be readily explained by starting from the same concepts as were developed in the second section of the present part, as applied to the discharge chamber; in fact, the presence of the dielectric along the path of the discharge was not considered at all.

In order to gain a deeper understanding of the nature of the succession of the sparks along the track, it is necessary to consider in addition the time development of the process. The leading front of the high-voltage pulse blows the column of electrons toward the positive electrode in such a way, that only in part of the spark gap is there a relic left of the direction of the registered particle. In this part of the spark gap where no electrons were left, the discharge develops in a direction close to that of the external field. In the case of smaller gaps distortions in the inclined tracks are observed near the positive electrode, and these cannot be attributed to the removal of the electron column [69].

It is seen from the foregoing that the size of the spark section in the direction of the external field depends on the steepness of the high-voltage pulse applied to the chamber plates. The steeper the front, the smaller the displacement of the column of electrons and the easier it is for the spark to follow the particle track. It has already been noted that this effect is observed best of all in chambers in which the distance between electrodes is large. In such chambers, first of all, the part of the gap from which the electrons are removed by the pulse, is small compared with the entire interelectrode distance, and second, at large values of d the capacitance of the chamber decreases, other conditions being equal, that is, the front of the pulse becomes steeper.

It is noted in [38] that the succession of the spark along the track in the spark chamber deteriorated in time. This is probably connected with the appearance of electronegative gases in the chamber.

Having surveyed the papers on discharge in spark chambers, let us compare the physical characteristics of these two instruments. First, discharge in spark chambers barely differ in their counting and time characteristics. Their similarity manifests itself also in the ability of registering with high efficiency charged-particle showers. Finally, the development of the discharge along the particle trajectory is not restricted to the discharge chamber alone, inclined discharges occur in all spark chambers if the front of the high-voltage pulse applied to the plates is sufficiently steep.

Usually the spark chambers described in the literature have small interelectrode gaps and relatively large capacitances, and the leads supplying the pulse have relatively large resistance and inductance; this causes the front of the high-voltage pulse on the plates of the spark chambers to collapse and consequently the sparks follow along the direction of the electric field. The presence of a dielectric between the discharge-chamber electrodes, which at one time seemed very important, is of no decisive significance for the succession of the spark along the track, although it does influence the character of the discharge and some properties of the chamber.

19. Spark Chamber in a Magnetic Field

In practice it is very important to know whether a spark chamber can operate in a magnetic field, and if so what are its characteristics under these conditions. A convincing answer, at least to the first question, is the photograph shown in Fig. 35, taken from [54]. In a 49-layer spark chamber, filled with a mixture of argon (70%) and helium (30%) and placed in a 13 kG magnetic field, we can trace readily the tracks of fast cosmic particles, and also the track of a slow electron. We see that in many places the electron track is directed along the electrodes, but this does not prevent us from determining its curvature.

The accuracy with which the curvature of a track in a spark chamber is determined depends on many parameters: the size of the gap, the clearing field, the magnetic field intensity, the direction of particle motion, etc. In particular, in [44], where a 46-layer spark chamber filled with neon or helium was used, the momentum of a 15-BeV particle in a magnetic

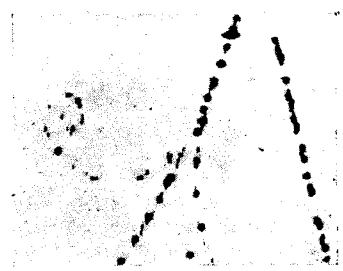

FIG. 35

field of 18 kG could be measured accurate to 1 per cent. In the same paper it is noted that the magnetic field did not noticeably influence the efficiency and other characteristics of the chamber. Somewhat more detailed data on the influence of the magnetic field on the spark-chamber characteristics are given in [47]. In particular, the so-called $\mathbf{E} \times \mathbf{B}$ effect is observed, consisting in the displacement of the primary-electron column by the action of the clearing electric field $\mathbf{E}$ and the magnetic field $\mathbf{B}$, and consequently a displacement of the spark channel relative to the place where the particle passes. Figure 36 shows a photograph of a track in a chamber with every other electrode connected to the power supply, so that the sparks were displaced in opposite directions in neighboring spark gaps. The displacement is proportional to E, B, and the time of action of these fields, that is, the time delay of the high-voltage pulse. The photograph shown was obtained with E = 100 V, B = 13 kG, and τ_d = 1 μsec. The displacement of the sparks is ~5 mm. The authors note that the memory time of the chamber has been increased. Such effects as the displacement and the smearing of the spark as a function of the current through the spark have not been investigated experimentally and are not considered here. What is striking is that in a magnetic field the observed shift of the sparks in a spark chamber filled with inert gas is much larger than in an air-filled spark counter (see Sec. 4 of Part II [30]). The very small deviations of the sparks in an air-filled spark chamber are connected apparently with the short lifetimes of the primary electrons produced on the path of the charged particle: within a time $<10^{-7}$ sec they stick to the oxygen molecules and their mobility drops sharply.

In ordinary spark chambers, the voltage pulse is applied 10^{-6} sec after the passage of the charged particle; during that time the primary electrons can move far away from their point of initiation in strong electric (E) and magnetic (B) fields.

20. Spark Chamber Constructions

There are various published descriptions of spark chambers, with constructions that differ greatly from one another. We shall attempt, however, to group them in several classes. The most frequently encountered spark-chamber construction is in the form of a rack of electrodes of alternating polarities. The electrodes are separated from one another by means of insulating adjusting washers [30,37,38], or else are alternately interconnected by metal posts in such a way that two racks, one inserted in the other, are produced [46]; in this case the electrodes of one polarity are turned 90° relative to the electrodes of the other polarity in the plane of the electrodes. The working part of the chamber is formed at the place where the electrodes cross. The entire construction is placed in one common evacuated volume with windows for photography. Figure 37 shows the photograph of such a chamber*.

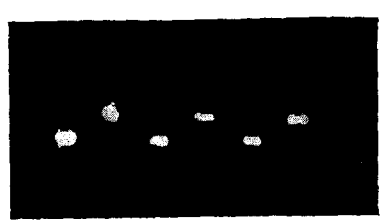

FIG. 36

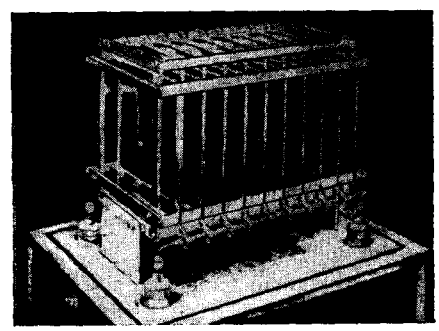

FIG. 37

Another class includes chambers made up of individual spark gaps. Frequently the spark gap is made in the form of a Plexiglas or glass frame, enclosed on both sides by plates—electrodes (for example [49,50]). This class usually includes track type chambers.

For some experiments it may be quite useful to employ a spark chamber in which a large solid angle is subtended [45]. The electrodes of this chamber are made in the form of coaxial cylinders, mounted between plexiglas flanges. A diagram of the chamber is shown in Fig. 39 below.

Special mention should be made of chambers with a minimum amount of matter along the particle path [48,55]. The authors of [55] constructed a four-layer chamber with electrodes made of thin aluminum foil, 7 μ thick, stretched over round frames. The chamber had windows for the passage of the particles, made of polyethylene film 70 μ thick. It was shown [48,55] that the damage produced to the foil by the sparks, namely pits, "craters," and even holes, does not change the chamber characteristics. Chambers of this type are necessary for experiments under conditions where the gamma background is large, and also where an appreciable role can be played by multiple scattering in the electrodes. Recently a "filament" spark cham-

*An interesting variant of this construction was demonstrated by A. A. Tyapkin at the 1961 Conference on Nuclear Radioelectronics in Moscow.

ber was reported [33].* In this instrument the spark jumps between oppositely charged filaments, arranged in a definite sequence. They can be stretched in different planes. We know little so far about this instrument, but it is assumed that it will find application where it is necessary to register particles moving in different directions or else along a trajectory with large curvature (spark chamber in a magnetic field). It is readily understood that in a filament spark chamber the problems involved in photography will be greatly simplified, particularly if the filaments can be made sufficiently thin.

The main difficulty in the construction of a spark chamber of any type is to overcome false breakdowns on the edges of the electrodes or through the Plexiglas wall between the electrodes. To eliminate false breakdowns in chambers of the "rack" type, the ends of the electrodes are rounded off, covered with insulating material, or enclosed in special jackets of insulating material. Sometimes the electrodes are shaped in such a way that their edges are farther from one another than the working surfaces of the electrodes.

Elementary cleanliness conditions must of course be observed in the assembly of the chamber.

There are apparently no limitations on the materials from which the electrodes are made. Brass, iron, aluminum, lead, glass with conducting coating, etc. have all been used. The housing of the chamber has been made of glass, Plexiglas, or metal. Packing of rubber and teflon was used in the chambers, and epoxy resins were used as glues. It must be noted that sometimes the chambers begin slowly to lose their efficiency, particularly in the registration of several particles. This effect depends, in the opinion of many authors, on the gas released from the walls of the chamber and the other structural elements (Plexiglas, rubber).

21. Effect of Additives in the Working Gas on the Characteristics of Spark Chambers

The effect of additives on the working characteristics was not investigated systematically so far. It is known, however, that the role of different additives, even in small concentrations, differs greatly both in character of their action and in the physical nature of the processes in which they participate.

In some investigations alcohol vapor was added to the neon or the argon filling the chamber. Such an addition improves the operation of the chamber [33,38] and reduces the number of the false sparks, which sometimes accompany the discharge along the particle track, but apparently calls for some increase in the working voltage. Other organic additives, such as acetone, dichloroethane, etc, act similarly. Their operating mechanism is connected with photon absorption and is well known from experience with Geiger counters.

The influence of additives that may enter the chamber during its production and operation was considered in [43,44]. First among these is air. It has been shown [43] that addition of air with partial pressure 0.02 mm Hg does not affect the efficiency of a spark chamber. When the partial pressure of the air in the chamber is 0.1 mm Hg, the efficiency decreases by less than 10 per cent. These data agree with the results of [36]. They are important for the determination of the vacuum required before filling the chamber. Upon further increase in the amount of air in the chamber, the efficiency of the latter decreases, owing to the production of electronegative molecules which do not disintegrate at the gradients under which spark chambers filled with inert gases operate.

Small additions of nitrogen and carbon dioxide have an effect similar to that of oxygen. It must be noted that in many investigations technical argon is used, which always contains some amounts of these gases.

The presence of water vapor in the gas of the chamber leads to the occurrence of false breakdowns at lower voltages, increases the probability of false breakdowns, and reduces somewhat the registration efficiency. These effects can apparently be connected with the dissociation of the water molecule.

It is interesting to note the effects produced on the operation of the chamber by the vapor of carbon tetrachloride, which is sometimes used in laboratory practice to wash equipment. The presence of even negligible amounts of carbon tetrachloride in the chamber reduces the chamber efficiency in the triggered mode at $\tau_d = 0.5$ sec to zero [43]; many hours of pumping are needed to restore the chamber efficiency.

Many spark chambers are filled with neon to which argon is added. The addition of a small amount of argon to the neon increases the ionization density, owing to the Penning effect.* The presence of metastable states of the atoms of inert gases can greatly influence the memory time of the chamber and its dead time. In this sense, a noticeable role can be played by additives which remove the excitation as a result of impact of the second kind.

Attention is called in [45] to the fact that small additions of xenon ($\sim 0.1\%$) to the neon increase the brightness of the sparks.

*There are also published descriptions of spark counters in which one of the electrodes is made in the form of several filaments stretched in one plane (see, for example [56], where all the earlier work is referred to).

*It is shown in [35] that the same Penning mechanism, which acts during the short time of spark development, reduces the operating potential. In chambers filled with neon and argon, the optimum argon concentration is 30 per cent.

22. Features of Photography of Particle Tracks in Discharge and Spark Chambers

The overall scheme for photographing particle tracks in a spark or discharge chamber is the same as in other track chambers. We emphasize below only those photography features connected with the specific nature of spark detectors.

The first distinguishing feature is that the object photographed is a spark. This solves completely the illumination problem of ordinary track chambers, which is frequently quite complicated. Usually the sparks are sufficiently bright (with the exception of some cases when the discharge develops between dielectric-coated electrodes), so that small diaphragms can be used, increasing the depth of focus and reducing the requirements with respect to lens quality. For the same reason, flashes and occasional extraneous illumination of the volume of the chamber present no danger.

A second feature pertains essentially to spark chambers with small interelectrode distances. If the chambers have any appreciable depth and consist of several spark gaps, then difficulties arise in the photography of the entire working volume with a single lens, since in ordinary photographic systems the opaque plates (electrodes) interfere with the photography. Consequently in many investigations the optical system of the spark chamber includes a cylindrical lens with generators parallel to the electrodes, and the camera is placed in the focus of the lens, which extends beyond the photographed volume [46]. A schematic diagram of such a system is shown in Fig. 38. In order to view the spark gaps over the entire depth of a cylindrical spark chamber, the authors of [45] used part of a spherical lens (Fig. 39).

Cylindrical lenses introduce certain distortion in the track images, and these are particularly important in precise measurements of the tracks in spark chambers. Some technical difficulties in the manufacture of good cylindrical lens for large chambers must be kept in mind.

If the spark chamber consists of individual spark gaps, then a possible method of photography is to arrange the photographic plates around the axis passing

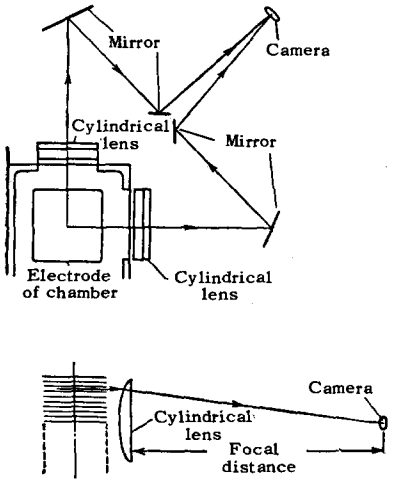

FIG. 38

through the lenses of two stereo cameras [55]. In view of the inclination of the gaps relative to one another, the volume of the chamber is used less effectively, but the tracks remain undistorted. In many investigations simple mirror systems are used to photograph the tracks in two projections on a single frame.

It must be noted that there are still no published papers in which the problem of photography of tracks in spark chambers and the concomitant errors are considered in sufficient detail.

23. Microwave Chamber

To conclude this chapter let us consider a microwave or highfrequency spark chamber. Strictly speaking, this is not even a spark-type particle detector. We consider it appropriate, however, to mention this new instrument, to which only a few papers have been devoted so far.

The microwave chamber is a cavity resonator filled with a Penning mixture (Ne + 0.5% Ar) at atmospheric pressure. At the instant of passage of the registered particles through the cavity volume, a pulse of microwave oscillation of 3000 Mc frequency and of $\sim 10^{-7}$ sec duration is excited in the cavity. The amplitude of the microwave oscillations is sufficient to permit the electrons produced along the path of the

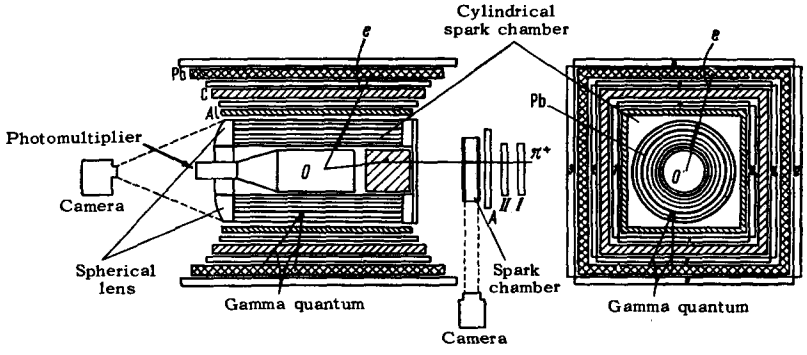

FIG. 39

Table VII

Track instruments	Spatial resolution, cm	Sensitivity time; sec	Can it be controlled?	Dead time, sec
Emulsions	10^{-4}	—	No	—
Cloud chamber	10^{-2}	10^{-2}	Yes	30
Bubble chamber	10^{-2}	$\sim 10^{-2}$	No	1
Spark chamber	$5 \cdot 10^{-2}$	$5 \cdot 10^{-7}$	Yes	10^{-2}

passing particle to multiply effectively and cause the gas to glow at their location. The authors of the papers have observed gas glow at the place of passage of the particle, but did not obtain satisfactory tracks as yet.

The microwave discharge chamber may have that advantage over ordinary spark or discharge chambers in that the maximum accuracy is the same in any direction.

The authors of [58] believe that further improvement in the microwave spark chamber will yield thinner tracks and better localization than obtained with ordinary spark or discharge chambers, since the electrons do not move far from the point of their initiation during the development of the discharge. It is also possible that the microwave discharge chamber will have better time resolution.

IV. APPLICATIONS OF DISCHARGE AND SPARK CHAMBERS

24. Comparison of Spark Chamber with Other Particle Detectors

Before we discuss the problems connected with the use of discharge and spark chambers, it is useful to summarize the main features of this instrument and to compare them with the properties of other widely used particle detectors.*

The spark chamber is a track instrument, which makes it possible to reconstitute the trajectory of the registered particle. In this respect it is similar to a cloud chamber and to the diffusion and bubble chambers. The ability to display and to provide recorded data distinguishes the spark chamber from such detectors as Geiger and scintillation counters. The accuracy of localization of the particles in the spark chamber (fractions of a millimeter) and the spatial resolution of several simultaneously traveling particles (not worse than 1 mm) are many times greater than the resolution of a hodoscope consisting of Geiger and scintillation counters.

On the other hand, the spark chamber is an electronic instrument with a time resolution on the order of fractions of a microsecond. Such times are characteristic of coincidence circuits using Geiger counters and is worse than the resolution times of modern scintillation-counter coincidence circuits by only a factor of several times ten. Thus, the spark chamber is incomparably better in its time characteristics than other track-type particle detectors. The spark chamber has a 100 per cent registration efficiency for charged particles. In this characteristic it is similar to other widely used radiation detectors. However, the spark chamber may turn out to be noticeably more effective than the latter for the registration of neutral radiation such as gamma quanta, neutrons, and neutrinos. This is connected with the fact that it is easy to construct spark chambers with a very large amount of matter along the particle path. The spark chamber can be made practically insensitive to neutral radiation, if its electrodes are made in the form of thin foils or screens of light material.

By its very nature, the spark chamber is a controllable chamber. This feature greatly determines the setup of the experiments. The chamber is usually combined with a more or less complicated electronic system, which selects from among many other events the particular one of interest to the experimenter. In other words, the spark chamber is not a global instrument like the bubble chamber, which registers all the phenomena occurring within its volume, but an instrument aimed principally at obtaining a preselected specific process.

Not the least important among the features of the spark chamber is the relative simplicity of the construction, even in the case when the dimensions are large. The simplicity of construction causes the spark chamber also to be relatively inexpensive, and consequently available to laboratories having small material and technical resources.

Some numerical characteristics of the spark chambers and other particle detectors are compared in Table VII.

25. Applications of Spark Chambers

Thus, the new instrument—spark chamber—combines to a considerable degree the features of a fast electronic and a track-type particle detector. Such a combination of the properties must be admitted to be very successful from the point of view of modern problems in experimental physics of high-energy particles.

*When we speak henceforth of spark chambers, we mean both discharge and spark chambers.

At the energies attained with accelerators, there is already sufficiently detailed information concerning the cross sections of the majority of the ordinary most probable processes. Attention is now focused on obtaining detailed characteristics of many low-probability processes. It becomes necessary in practice to distinguish the process of interest against a large background of accompanying processes, which frequently are tens of thousands of times larger than the effect itself. For this purpose it is necessary to introduce a maximum number of selection criteria for the specified event, and when working by the scintillation technique it is necessary in addition to set up laborious and prolonged background experiments.

A photograph of a process contains much information about the various events. This is one of the reasons why many of the rather interesting investigations have been carried out recently with bubble chambers. There is no doubt that the limits of the capabilities of this widely used instrument have not yet been reached. For many physical problems, however, the sensible limit of applicability of the bubble chamber has already been reached. We refer to the observation of such rare processes, yet those growing in importance from day to day, wherein 10—15 selected events are selected from 5×10^5—10^6 photographs made in a large bubble chamber. In such cases the production of the photographs and particularly the selection consume very much time, even if the particle tracks on the photographs are processed by modern machine methods.

A photograph can be readily processed if it contains not more than 20—40 incoming particles. If the number of photographs is 10^6, the total flux of particles registered in a bubble chamber cannot exceed $(2—4) \times 10^7$ particles. This means that in many cases the chamber procedure makes inefficient use of the particle fluxes in existing proton accelerators. In fact, in principle, electronic registration methods make it possible to accumulate adequate statistics for proton beams during one accelerator pulse, and for pion beams in approximately one hour of operation. Another advantage of electronics is the possibility of selecting the particles by their velocities (Cerenkov counters), so that the particle masses can be determined if the momenta are known. On the other hand, in bubble chambers, relativistic particles have tracks which hardly differ from one another.

Nevertheless, as noted above, electronic methods have a major shortcoming, namely the lack of direct registration and low reliability of each individual event. A unique vicious circle is produced, a way out of which is to use the spark-chamber procedure.

The scheme of the experiment is as follows. An electronic system consisting of scintillation and Cerenkov counters, connected for coincidence and anticoincidence, identifies the beam particles and the secondary particles—the products of the investigated nuclear reaction. The interaction occurs either inside the spark chamber, or else the secondary particles pass through its spark gaps. If the criteria set by the electronic system are satisfied, a pulse is produced and causes operation of the spark chamber. The experimenter acquires a photograph of an event separated in the spark chamber itself with a time resolution of ~ 1 sec, that is, against the background of a beam of particles having an intensity 10^6 particles/sec.

In this connection it must be emphasized that the spark chamber can be used in individual cases very effectively to study a definite nuclear reaction, whereas the bubble chamber makes it possible to discover interactions having heretofore unknown properties (production and decay of new particles, etc). It is clear that the spark chamber certainly does not "replace" the bubble chamber (or any other instrument used in high-energy particle physics).

The idea of using these instruments simultaneously has been advanced recently. A spark chamber preceding a bubble chamber is operated by a pulse from an electronic circuit that separates the specified particle (say an antiproton in a pion beam) and indicates which of the tracks in the bubble chamber belongs to the selected particle. Analogously, a spark chamber can be combined with a nuclear emulsion [60].

Let us proceed to consider some specific experiments.

One of the first applications of the spark chamber with an accelerator was the measurement of proton polarization in elastic π^-p scattering in the region of the second (600 MeV) and third (880 MeV) pion-nucleon resonances. It is well known that in order to determine the beam polarization it is necessary to measure the right-left asymmetry which occurs upon secondary scattering of the beam. The need for observing second scattering greatly reduces the efficiency of the ordinary methods of investigation of polarization. The experimental setup of Cork et al [61] using a spark chamber is shown in Fig. 40. The scintillation and Cerenkov counters, connected in a coincidence-anticoincidence $1 + 2 + 3 + 4 + 5 - 6$ circuit, separate those elastic π^-p scattering events on a polyethylene target, wherein the scattered proton is

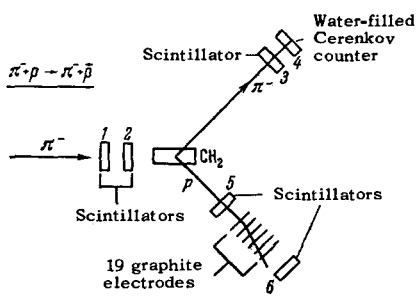

FIG. 40

scattered again in the graphite plates of the spark chamber and is not registered by counter 6. Photography of the secondary scattering in the plates of the spark chamber, operated by a pulse from the electronic circuit, makes it readily possible to find the ratio of the number of particles scattered to the right and to the left relative to the direction of motion of the protons. We emphasize that in the registration of the secondary scattering, practically the entire solid angle is encompassed. Six non-physicists processed the 100,000 obtained photographs in one month.

An analogous setup, including two spark chambers in which the secondary scattering of both scattered particles was measured, was used by Cronin et al [62] to investigate spin-spin correlation in elastic pp scattering.

An interesting example of the use of a spark chamber for the investigation of a rare decay is provided by the experiments on the search for the $\mu \rightarrow e + \gamma$ process, carried out by Alikhanov, Babaev, et al [63]. A six-layer cylindrical spark chamber was used, operated by a signal fed from scintillation counters, connected for $0 + 4 + 5 + 7 + 8 - 6 - 9 - A$ and $0 + 1 + 2 + 10 + 11 - 3 - 12 - A$. A diagram of the setup is shown in Fig. 39. The first four spark gaps were used to register the electron, and the last two, which were beyond the lead converter, registered in addition to the electron also the electron-positron pair from the gamma-quantum conversion. The electron and the gamma quantum from the decay of the resting muon scattered in opposite directions, as could readily be established with the aid of the spark chamber. The use of such an additional criterion in the selection of the $\mu \rightarrow e + \gamma$ events has made it possible for the authors to reduce the upper limit of the probability of the obtained reaction by a factor of several times compared with the earlier electronic experiments, to a value 5×10^{-7} with 90 per cent confidence.*

Figure 41 shows the diagram of another experiment [65] where a spark chamber was used. The apparatus is used to investigate the $\pi^- + p \rightarrow \pi^- + \pi^+ + n$ reaction with small momentum transfer to the nucleon, in order to obtain information on the $\pi\pi$ interaction. A high-voltage pulse is applied to the spark chamber if the pion leaves the beam, and simultaneously two telescopes which register the scattered particles operate. The photography of the event in a spark chamber makes it possible to employ several additional selection critieria and to determine with sufficient accuracy the angles of emission of the secondary particles. In order to measure more accurately the angles and to avoid conversion of the background gamma quanta in the electrode plates, the latter are made of aluminum foil.

There are reports in the literature of a successful

*Recently[64] this limit was reduced to 6×10^{-8}.

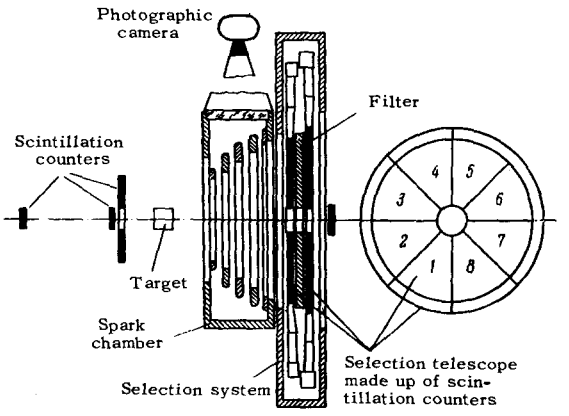

FIG. 41

application of spark chambers for the measurement of the asymmetry in the decays $\Sigma^+ \rightarrow n + \pi^+$ and $\Lambda^0 \rightarrow p + \pi^-$ [66] and the investigation of the Compton effect on protons and deuterons [67]. Rather obvious suggestions have been published concerning the use of large spark chambers with thick iron electrodes for the registration of neutrons [33]. In the 1961 Conference on Cosmic Rays in Japan, it was reported that the Fukui and Mijamoto discharge chamber was used in cosmic-ray experiments made on airplanes[68]. In these experiments, an additional advantage of the instrument is its low weight.

The prospects of the use of spark chambers for the study of cosmic rays are connected in particular with the fact that this relatively simple triggered track-type particle detector, with good spatial resolution, can be made with large dimensions.

Our examples do not exhaust, of course, all the experimental capabilities of the new instrument. The list presented is but a small fraction of those experiments in which the spark chamber will be used and is already being used.

[1] J. W. Keuffel, Phys. Rev. 73, 531 (1948).
[2] J. W. Keuffel, Rev. Sci. Instr. 20, 202 (1949).
[3] J. Christiansen, Z. angew. Phys. 4, 326 (1952).
[4] J. M. Meek and J. D. Craggs, Electrical Breakdown of Gases, Oxford Univ. Press, 1953.
[5] N. A. Kaptsov, Elektricheskie yavleniya v gazakh i vakuume (Electric Phenomena in Gases and Vacuum), Gostekhizdat, 1947.
[6] L. Loeb, Fundamental Processes of Electrical Discharge in Gases, Wiley, N. Y., 1939.
[7] L. Madansky and R. W. Pidd, Phys. Rev. 73, 1215 (1948).
[8] L. Madansky and R. W. Pidd, Phys. Rev. 75, 1175 (1949).
[9] E. Robinson, Proc. Phys. Soc. A66, 73 (1953).
[10] P. G. Henning, Atomkern-Energie 2, 81 (1957).
[11] L. Madansky and R. W. Pidd, Rev. Sci. Instr. 21 (5), 407 (1950).

[12] Bella, Franzinetti, and Lee, Nuovo Cimento 10(9), 1338 (1953).
[13] E. Bagge and O. C. Allkofer, Atomkern-Energie 2(1), 7 (1957).
[14] E. Bagge and L. Schmieder, Atomkern-Energie 4(5), 169 (1959).
[15] O. C. Allkofer, Atomkern-Energie 4(10), 389 (1959).
[16] H. Raether, Ergebn, exakt. Naturwiss. 22 (1949).
[17] Babykin, Plakhov, Skachkov, and Shapkin, Atomnaya énergiya No. 4, 38 (1956).
[18] E. K. Zavoĭskiĭ and G. E. Smolkin, Atomnaya énergiya, No. 4, 46 (1956).
[19] Yu. F. Skachkov, PTÉ, No. 6, 41 (1961).
[20] J. Trümper, Atomkern-Energie 5(4), 121 (1960).
[21] E. Robinson, Proc. Phys. Soc. A66, 79 (1953).
[22] Allkofer, Bagge, Henning, and Schmieder, Atomkern-Energie, 2, 88 (1957).
[23] O. C. Allkofer, Z. Phys. 158, 274 (1960).
[24] T. E. Cranshaw and I. F. de Beer, Nuovo cimento 5, 1107 (1957).
[25] M. Conversi and A. Gozzini, Nuovo cimento 2, 189 (1955).
[26] Conversi, Focardi, Franzinetti, Gozzini, and Murtas, Nuovo cimento, Suppl. al 4, 234 (1956).
[27] A. A. Tyapkin, PTÉ, No. 3, 51 (1956).
[28] V. V. Vishnyakov and A. A. Tyapkin, Atomnaya énergiya 3 (10) 298 (1957).
[29] G. Charpak, Paper at International Conference on the Experimental Methods of High-Energy Particle Physics, Geneva, 1962.
[30] Daĭon, Volynskiĭ, and Potapov, PTÉ, No. 2, 47 (1961).
[31] Bayukov, Leksin, and Suchkov, PTÉ, No. 3, 66 (1961).
[32] M. I. Daion, DAN SSSR 14 (3), 305 (1949).
[33] Spark Chamber Symposium, Rev. Sci. Instr. 32(5), 480 (1961).
[34] M. Thompson and A. W. Wolfendale, Nuovo cimento, Suppl. al 23(1), 144 (1962).
[35] S. Fukui and S. Mijamoto, Nuovo cimento 11(1), 113 (1959); Preprint Nr. 888, 1959.
[36] Mikhaĭlov, Roinishvili, and Chikovani, PTÉ, No. 1, 39 (1961).
[37] Volynskii, Daion, and Ponosov, PTÉ, No. 3, 155 (1961).
[38] Borisov, Dolgoshein, Luchkov, Reshetin, and Ushakov, PTÉ, No. 1, 49 (1962).
[39] Proceedings of an International Conference on Instrumentation for High-Energy Physics, N. Y.—London, September 1960.
[40] G. Charpak, J. phys. et radium. 18, 539 (1957).
[41] Fukui, Hayakawa, Kayiakawa, and Kikuchi, J. Phys. Soc. Japan 16, 2069 (1961).
[42] Govorov, Nikonorov, Peter, Pisarov, and Poze, PTÉ, No. 6, 49 (1961).
[43] Bayukov, Leksin, Suchkov, and Telenkov. Fifth Conference on Nuclear Radioelectronics, Moscow, 1961; PTÉ, No. 1, 36 (1963).
[44] G. K. O'Neill, Rev. Sci. Instr. 32, 5, 528 (1961).
[45] V. S. Kaftanov and V. A. Lyubimov, Nucl. Instr. Met. 20 (1963).
[46] J. W. Cronin and G. Renninger, Proceedings of an International Conference on Instrumentation for High-Energy Physics, 1960, 271.
[47] Beall, Cork, Murphy, and Wentzel, Proceedings of an International Conference on Instrumentation for High-Energy Physics, 1960, 277.
[48] J. Fischer and G. T. Zorn, Rev. Sci. Instr. 324(5), 499 (1961).
[49] D. J. Meyer and K. M. Terwilliger, Rev. Sci. Instr. 32(5), 512 (1961).
[50] J. G. Rutherglen and J. M. Paterson, Rev. Sci. Instr. 32(5), 522 (1961).
[51] J. G. Rutherglen and J. M. Paterson, Rev. Sci. Instr. 32(5), 519 (1961).
[52] Borisov, Dolgoshein, and Luchkov, PTÉ, No 2, 170 (1962).
[53] Mikhaĭlov, Roinishvili, and Chikovani, Fifth Conference on Nuclear Radioelectronics, Moscow, 1961.
[54] Burleson, Roberts, and Romanovski, Rev. Sci. Instr. 32(9), 1069 (1961).
[55] Bayukov, Leksin, Suchkov, and Telenkov, PTÉ, No. 2, 45 (1963).
[56] Mistry, Murthy, Murthy, and Sreekantan, Nuovo cimento 17(3), 429 (1960).
[57] Fukui, Hayakawa, Tsukishima, and Nukushina, Proceedings of an International Conference on Instrumentation for High-Energy Physics, 1960, 267.
[58] S. Fukui and S. Hayakawa, J. Phys. Soc. Japan 15, 532 (1960).
[59] L. M. Lederman, Rev. Sci. Instr. 32(5), 525 (1961).
[60] M. I. Daĭon and V. Kh. Volynskiĭ, JETP 37, 906 (1959), Soviet Phys. JETP 10, 648 (1960).
[61] B. Cork et al., Rev. Sci. Instr. 32(5), 486 (1961).
[62] Cronin, Bowen, Eugls et al., Rev. Sci. Instr. 32(5), 488 (1961).
[63] Alikhanov, Babaev, Balats, Kaftanov, Landsberg, Lyubimov, and Obukhov, JETP 42, 630 (1962), Soviet Phys. JETP 15, 438 (1962).
[64] Bartlett, Devons, and Sachs, Phys. Rev. Letts. 8(3), 120 (1961).
[65] Aref'ev, Bayukov, Zaĭtsev, Kozodaev, Leksin, Osipenkov, Suchkov, Telenkov, and Fedorov, Preprint, Inst. Theoret. and Exptl. Phys., 1962.
[66] Beall, Cork, Keefe, Murphy, and Wentzel, Phys. Rev. Letts. 7(7), 285 (1962).
[67] W. B. Hauson and L. Criege, Rev. Sci. Instr. 5(3), 494 (1961).
[68] Imai, Kamata, Kawasaki, and Murakami, Sci. Papers IPCR 55(1) (1961).
[69] A. A. Tyapkin and Tsou Chu-liang, Preprint, Joint Inst. Nuc. Res. D-870 (1962).

Translated by J. G. Adashko
24